Sestrin2 acts as a negative regulator of inflammasome activation by inducing mitophagy

Min-Ji Kim

Department of Medical Science

The Graduate School, Yonsei University

Sestrin2 acts as a negative regulator of inflammasome activation by inducing mitophagy

Directed by Professor Ji-Hwan Ryu

The Doctoral Dissertation
submitted to the Department of Medical Science,
the Graduate School of Yonsei University
in partial fulfillment of the requirements for the degree
of Doctor of Philosophy

Min-Ji Kim

December 2014

This certifies that the Doctoral Dissertation of Min-Ji Kim is approved.

Thesis Supervisor : Ji-Hwan Ryu

Thesis Committee Member#1: Sang Sun Yoon

Thesis Committee Member#2: Je-Wook Yu

Thesis Committee Member#3: Young Sam Kim

Thesis Committee Member#4: Seok Min Jin

The Graduate School
Yonsei University

December 2014

ACKNOWLEDGEMENTS

I really would like to thank my supervisor Professor Ji-Hwan Ryu for his great support, encouragement and advice throughout my PhD research studies. And I would like to express my special gratitude to Professor Joo-Heon Yoon for giving me an opportunity to work for the Research Center for Human Defense System and encouraging me all the time. I am also very grateful to the members of my PhD committee, Professors Sang Sun Yoon, Je-Wook Yu, Young Sam Kim and Seok Min Jin for their helpful advice and suggestions. My sincere thanks also goes to my collaborator Professor Soo Han Bae for his useful discussions.

I also have to thank all of the helpful and friendly collegues of my lab including Professors Chang-Hoon Kim, Hyun-Jik Kim, Dr.Sang-Nam Lee, Dr.Kyu-Nam Cho, Yungeun, Gahee, Jae-Chan, Younghee, Haegi, John, and my old collegues Dr.Jeong-Hee Joo and Jeong-Yeon.

I appreciate to Dr.Dong-Soo Jang for his amazing support with medical illustration. I really enjoyed working with him.

I am deeply indebted to my friends Sang-A, Saerom and Myong-Jin for their wonderful generosity and friendship.

Most importantly, I would like to thank all my family especially my grandmother, parents, sister and nephew for their continued support, encouragement and unconditional love.

TABLE OF CONTENTS

LIST OF FIGURES

ABSTRACT

Sestrin2 acts as a negative regulator of inflammasome activation by inducing mitophagy

Min-Ji Kim

Department of Medical Science
The Graduate School, Yonsei University

(Directed by Professor Ji-Hwan Ryu)

In “danger” conditions, such as infections, the NLRP3 inflammasome complex is positively regulated by mitochondria-generated reactive oxygen species and negatively regulated by autophagy. Thus, tight regulation of both mitochondrial integrity and autophagy is essential for proper inflammasome activation. Here, I demonstrate that Sestrin2 suppressed continuous inflammasome activation by preserving mitochondrial homeostasis through inducing selective autophagy. Sestrin2 plays a dual role to remove damaged mitochondria caused by stimulation with LPS and ATP in macrophages. First, Sestrin2 facilitates the perinuclear clustering of damaged mitochondria by mediating aggregation of p62/SQSTM1 and its recruitment to Lys 63 ubiquitins on mitochondria surface. Second, Sestrin2 induces autophagosome formation and mitophagy through maintenance of ULK1 stability. Thus, both Sestrin2- and p62-deficient mice had more damaged mitochondria, and

produced more caspase-1-dependent cytokines, including IL-1β and IL-18, and had higher mortality in sepsis models. These findings identify a novel role of Sestrin2 and p62 for protection against incessant inflammation.

Key words : Sestrin2, p62, Autophagy, Mitophagy

Sestrin2 acts as a negative regulator of inflammasome activation by inducing mitophagy

Min-Ji Kim

Department of Medical Science
The Graduate School, Yonsei University

(Directed by Professor Ji-Hwan Ryu)

I. INTRODUCTION

The vertebrate immune system employs a variety of sensors to recognize pathogens or tissue damage, and trigger innate immune responses for host defense. Nod-like receptors (NLRs) are a group of cytosolic proteins that detect and are activated by a variety of danger signals, including pathogen associated molecular patterns (PAMPs) and host-derived molecules generated by cellular damage[1,2]. NLRP3, the best studied of the NLRs, is the main component of the multi-protein signaling complex called the inflammasome, which is formed upon NLRP3 stimulation by various pathogens[3-5]. Upon activation, NLRP3 oligomerizes with the apoptosis-associated adaptor protein ASC and pro-caspase-1, which results in caspase-1 activation, leading to cleavage of the proforms of IL-1β and IL-18 to produce the active cytokines[6,7]. Although the specific molecules and mechanisms which trigger NLRP3 inflammasome activation are currently unclear, one commonly proposed mechanism is induction by reactive oxygen species (ROS) generation[8,9]. Recently, several reports have shown that ROS or oxidized mitochondrial

DNA generated from damaged midtochondria activate the NLRP3 inflammasome[10-13]. Although mitochondrial ROS induced by NLRP3 activators is critical for inflammasome activation, perpetual inflammasome activation under chronic mitochondrial injury might prove catastrophic for immune homeostasis. Thus, there is a need for cleaning systems to remove damaged mitochondria in order to dampen incessant inflammasome activation. Recently, in autophagy regulator ATG16L1 deficient mice, excessive amounts of IL-1β and IL-18 were produced by immune stimulation, probably as a consequence of enhanced inflammasome activation[14]. Furthermore, it has been reported that autophagic proteins suppress inflammasome activation through preservation of mitochondrial integrity[11,15]. However, the regulatory mechanisms whereby autophagy is initiated by immune stimulator and how activated autophagy maintains mitochondrial homeostasis through clearance of damaged mitochondria remain largely unknown.

Sestrins (Sesns) are highly conserved proteins that protect cells exposed to a variety of environmental stresses, including oxidative stress and DNA damage[16,17]. Despite their significance, the biochemical functions of Sesns are not well understood, because the proteins do not have any structural domains or catalytic motifs known to be responsible for specific functions. However, it has recently been found that Sesn2 is necessary to protect cells from oxidative stress through binding to Keap1 (Kelch-like ECH-associated protein 1) and p62/SQSTM1 (hereafter referred to as p62), thereby inducing autophagic degradation of Keap1 and subsequent activation of NRF2 (Nuclear factor erythroid 2-related factor 2)[18]. Apart from their roles as antioxidants against oxidative stress, Sesn2, Sesn3, and *Drosophila* Sesn maintain metabolic homeostasis through induction of AMPK activation and subsequent suppression of mTORC1 activity[17,19-21]. Furthermore, recent results obtained from mice deficient in Sesn2 support a protective role of Sesns in regulation of endoplasmic reticulum (ER) stress[22]. Despite significant progress in

understanding the functions of Sesns in metabolic pathways and diseases, the regulatory roles of Sesns in immune responses and the mechanisms involved therein have not yet been revealed. Here, I describe a novel role for Sesn2 in the suppression of excessive inflammasome activation by preserving mitochondrial integrity via autophagy initiation and mitophagy activation.

II. MATERIALS AND METHODS

1. Mice

Sesn2$^{-/-}$ and p62$^{-/-}$ mice were kindly provided by Dr. Rhee of Yonsei University and Dr. Shin of Sungkyunkwan University, respectively. All mice were 12-16 weeks of age at use. Mice were maintained in specific pathogen-free conditions. All animal experiments and protocols were approved by the Yonsei University College of Medicine institutional animal care and use committee.

2. Cell Culture and Treatment

Bone marrow-derived macrophages (BMDMs) were cultured in MEM-alpha with 10% fetal bovine serum and 20 ng/ml M-CSF (R&D Systems, Minneapolis, MN, USA). Fresh medium was added on day 3 and macrophages were used after 5 days of culture. Cells were primed with LPS (100 ng/ml) for 6 h, 12 h, or 24 h, and treated with ATP (1 mM) for 30 minutes. To inhibit mitochondrial ROS, Mito-TEMPO (Enzo Life Science, Farmingdale, NY, USA) was administered and cells were pre-incubated for 1 h prior to LPS treatment. Cells were treated with 5uM of nigericin (Sigma, St.Louis, MO, USA) for 45 minutes, 12 h after LPS priming, and 1 ug/ml of poly dAdT was transfected with LPS for 12 h. Peritoneal macrophages were prepared as described previously, with some modifications (Nakahira et al., 2011). Briefly, peritoneal macrophages were elicited with 1 ml of 3% (vol/vol) thioglycolate solution and were collected by peritoneal lavage 3 days later. After 2 h of incubation, non-adherent cells were removed. Cells were primed with LPS (200 ng/ml) for 6 h, or 12 h and treated with ATP (2 mM) for 30 minutes.

3. Flow Cytometry

Mitochondrial ROS were measured by staining cells with MitoSOX

(Invitrogen, Carlsbad, CA, USA) at 5 uM for 15 min at 37℃. To measure mitochondrial mass, cells were stained with MitoTracker Green FM and MitoTracker Deep Red FM (Invitrogen, Carlsbad, CA, USA) at 25 nM for 15 min at 37℃. Cells were then washed with PBS, trypsinized and resuspended in cold PBS containing 1% FBS. To check the purity of isolated monocytes from human blood, CD14-FITC (Miltenyi Biotec, Bergisch Gladbach, Germany) was used. Data were acquired and analyzed with a BD LSR II flow cytometer (BD Biosciences, San Jose, CA, USA).

4. Transmission Electron Microscopy

BMDMs were fixed with glutaraldehyde as described previously (Shin et al., 2010).

5. ELISA

Cell culture supernatants and serum were assayed by ELISA for IL-1β (R&D Systems, Minneapolis, MN, USA), TNF (R&D Systems, Minneapolis, MN, USA) and IL-18 (MBL, Nagoya, Japan).

6. Immunoblotting and Immunoprecipitation

The following primary antibodies were used: Sesn2 (10795-1-AP; ProteinTech, Chicago, IL, USA), p62 (H00008878-M01; Abnova, Taipei, Taiwan), IL-1β (5129-100; Biovision, Mountain view, CA, USA), Caspase-1 (sc-514; Santa Cruz, Santa Cruz, CA, USA), NLRP3 (AG-20B-0014-C100; Adipogen), P2X7 (APR-004-AO; Alomone Labs), ASC (sc-22514-R; Santa Cruz, Santa Cruz, CA, USA), AMPKα (2532; Cell Signaling, Danvers, MA, USA), phospho-AMPKα (2535; Cell Signaling, Danvers, MA, USA), S6 (2317; Cell Signaling, Danvers, MA, USA), and phopho-S6 (2211; Cell Signaling, Danvers, MA, USA), LC3B (L7543; Sigma, St.Louis, MO, USA), Caspase-3 (9662, Cell signaling, Danvers, MA, USA), Vdac1 (ab14734;

Abcam, Cambridge, UK), Beclin1 (3495; Cell signaling, Danvers, MA, USA), Atg5 (12994; Cell signaling, Danvers, MA, USA), Atg7 (8558; Cell signaling, Danvers, MA, USA), mouse ULK1 (A7481; Sigma, St.Louis, MO, USA), human ULK1 (sc-33182; Santa cruz, Santa Cruz, CA, USA), phospho-ULK1 S555 (5869; Cell Signaling, Danvers, MA, USA), phospho-ULK1 S757 (6888; Cell Signaling, Danvers, MA, USA), ULK2 (AAM80; AbD Serotec, Oxford, UK), Total IκBα (9242; Cell signaling, Danvers, MA, USA), phospho-IκBα (9246; Cell signaling, Danvers, MA, USA). β-actin (sc-47778; Santa Cruz, Santa Cruz, CA, USA) was used as a loading control. Secreted proteins in the cell culture supernatants were precipitated by methanol/chloroform precipitation. Cells were lysed with lysis buffer (Invitrogen, Carlsbad, CA, USA). Lysates were boiled 5 min in SDS-sample loading buffer and separated by SDS-PAGE, transferred to PVDF (Bio-Rad, Hercules, CA, USA), and incubated with primary antibodies followed by HRP-conjugated secondary antibodies. The blot was visualized using the ECL system (Thermo Fisher Scientific, Wyman Street Waltham, MA, USA). For immunoprecipitation, cell lysates were incubated with the appropriate primary antibodies overnight and then incubated with protein G-agarose (Sigma, St.Louis, MO, USA) for 2 h with gentle rotation at 4℃. The immunoprecipitates were washed five times with lysis buffer and boiled in SDS-loading buffer, then separated by SDS-PAGE and analyzed by immunoblotting.

7. Mitochondria/Cytosol fractionation

Mitochondrial fractions were obtained from BMDM using a Qproteome Mitochondria Isolation Kit (Qiagen, Valencia, CA, USA) following the manufacturer's instructions with minor modifications. Briefly, 5 x 10^6 cells were suspended in lysis buffer and incubated on an end-over-end shaker for 10 min at 4℃ and centrifuged at 1,000 x g for 10 min at 4℃. The pellet was resuspended in Disruption Buffer, passed 10 times through a 26 gauge needle

to ensure complete cell disruption, and centrifuged at 1,000 x g for 10 min at 4℃. The supernatant was centrifuged at 6,000 x g for 10 min at 4℃ to pellet mitochondria. The mitochondria were washed with Mitochondria Storage Buffer and centrifuged at 6,000 x g for 20 min at 4℃. The pellet was resuspended in an appropriate amount of Mitochondria Storage Buffer and the concentration was determined with a BCA protein assay kit (Thermo Fisher Scientific, Wyman Street Waltham, MA USA). Five to ten μg of mitochondrial proteins were used for immunoblotting.

8. Animal experiments

Male or female mice were injected with 12 mg/kg of *E. coli* LPS or its solvent (PBS) intraperitoneally before measuring serum cytokines. Blood samples were collected from mice via cardiac puncture. For endotoxic shock experiments, 25 mg/kg of LPS were injected intraperitoneally and survival rates were monitored for 1 week. For 'add-back' rescue, adenoviruses (Ad) encoding Sesn2 (Ad-Sesn2), Ad encoding p62 (Ad-p62), and Ad Control (Ad-Cont) were obtained from Seoulin Bioscience. Adenoviruses (5×10^9 viral particles) were injected intravenously 48 h before LPS challenge.

9. Immunofluorescence Staining and Confocal Microscopy

Cells seeded on glass coverslips were treated with LPS and ATP, followed by fixation and permeabilization with methanol for 10 min at room temperature. After washing cells with PBS three times, cells were blocked with 1% BSA in antibody diluent (Dako, Glostrup, Denmark) for 1 hr at room temperature. They were then incubated overnight with primary antibodies in antibody diluent at 4℃. After washing cells with PBS three times, cells were incubated with secondary antibodies for 30 min at room temperature. Finally, cells were washed with PBS three times and stained with 4', 6'-diamidino-2-phenylindole (DAPI, Sigma, St.Louis, MO, USA) for 2 min at

room temperature. Cells were then washed with PBS, mounted onto slides with mounting medium and observed on an LSM700 confocal microscope (Carl Zeiss, Jena, Germany) at 800x magnification. The following antibodies were used: Sesn2 (Abclon, Seoul, Korea), p62 (H00008878-M01; Abnova, Taipei, Taiwan) and Tom20 (sc-11415; Santa Cruz, Santa Cruz, CA, USA), Lys63-linked ubiquitin (05-1308; Millipore, Billerica, MA, USA), Lys48-linked ubiquitin (05-1307; Millipore, Billerica, MA, USA) as primary antibodies, and Alexa 488 (Molecular Probes, Eugene, Oregon**,** USA) and Alexa 568 (Molecular Probes, Eugene, Oregon**,** USA) as secondary antibodies. To perform the Proximity Ligation Assay (PLA), Duolink II PLA probes and Detection Reagents (Olink Bioscience, Uppsala, Sweden) were used following the manufacturer's instructions. The nuclei were counterstained with DAPI and PLA signals were visualized on a confocal microscope at 800 x magnification. Cells with punctuated GFP-LC3 were counted manually following a method described previously[23].

10. Human study

Human blood samples from healthy volunteers and septic shock patients were obtained in Severance Hospital (Korea). This study was approved by Institutional Review Board of Severance Hospital, Yonsei University College of Medicine, (4-2013-0585). Peripheral blood mononuclear cells were separated by Ficoll density gradient centrifugation. Aliquots of plasma were stored at -80℃ and monocytes were isolated from buffy coats and enriched by depletion using a Monocyte Isolation Kit II (Miltenyi Biotec, Bergisch Gladbach, Germany).

11. Retroviral overexpression of GFP-LC3 and human ULK1

GFP-LC3 and HA-tagged human ULK1 pRK5 plasmid were obtained from Addgene and were originally deposited by Tamotsu Yoshimori (The National Institute of Genetics, Japan) and Dr. Do-Hyung Kim (University of

Minnesota, USA), respectively. The GFP-LC3 and ULK1 insert were cloned into the LZR retroviral vector and retroviral particles were produced in HEK293 GPG packaging cells. The LZR retroviral vector and HEK293 GPG packaging cells were kindly gifted by Dr. Jaesang Kim (Ewha Womans University, Korea). Target cells were infected with retroviral particles after 3 days of culture and incubated for an additional 2 days.

12. Statistical Analysis

An unpaired Student's *t* test was performed for the Comparison of two samples and ANOVA was performed for the Comparison of multiple samples. The Kaplan-Meier log-rank test was used for the statistical analysis of survival experiments. p values < 0.05 were considered statistically significant. SPSS software (Chicago, IL, USA) was used for all analyses.

III. RESULTS

1. Sesn2 serves a protective role against septic shock in mouse sepsis models

To examine the potential role of Sesn2 in the immune response to septic shock, I employed endotoxemic mice, which are generally used as a model of septic shock. First, I assessed whether Sesn2 deficiency affected susceptibility to endotoxemia induced by intraperitoneal injection with LPS. Relative to wild-type controls ($Sesn2^{+/+}$), $Sesn2^{-/-}$ mice had significantly higher mortality rates (Figure 1A). Consistent with these findings, serum concentrations of IL-1β and IL-18 were higher in endotoxemic $Sesn2^{-/-}$ than in $Sesn2^{+/+}$ (Figure 1B). To confirm that the above pathological consequences in endotoxemic $Sesn2^{-/-}$ are attributable to deficiency of Sesn2 itself, I examined the recue effect of Sesn2 through intravenous injection of an adenoviral vector containing the human Sesn2 gene (Ad-Sesn2) into $Sesn2^{-/-}$ mice. I verified that Sesn2 expression in liver was detectable following injection with Ad-Sesn2, but not Ad-control (Ad-Cont) (Figure 1C). 'Add-back' rescue with Sesn2 significantly improved the survival of $Sesn2^{-/-}$ in endotoxemia (Figure 1D). In accordance with the results of survival rates, serum concentrations of IL-1β and IL-18 were decreased by rescue with Ad-Sesn2 (Figure 1E). Similar to the results obtained with the endotoxemia model, $Sesn2^{-/-}$ had higher mortalities and serum concentrations of IL-1β and IL-18 in Cecal ligation puncture(CLP)-induced sepsis (Figures 1F and 1G). Rescue with Sesn2 improved the survival rate and decreased the serum concentrations of IL-1β and IL-18 in CLP-induced $Sesn2^{-/-}$ (Figures 1H and 1I). These data indicate that Sesn2 has an essential role in protecting against two septic shock models including endotoxemia and CLP.

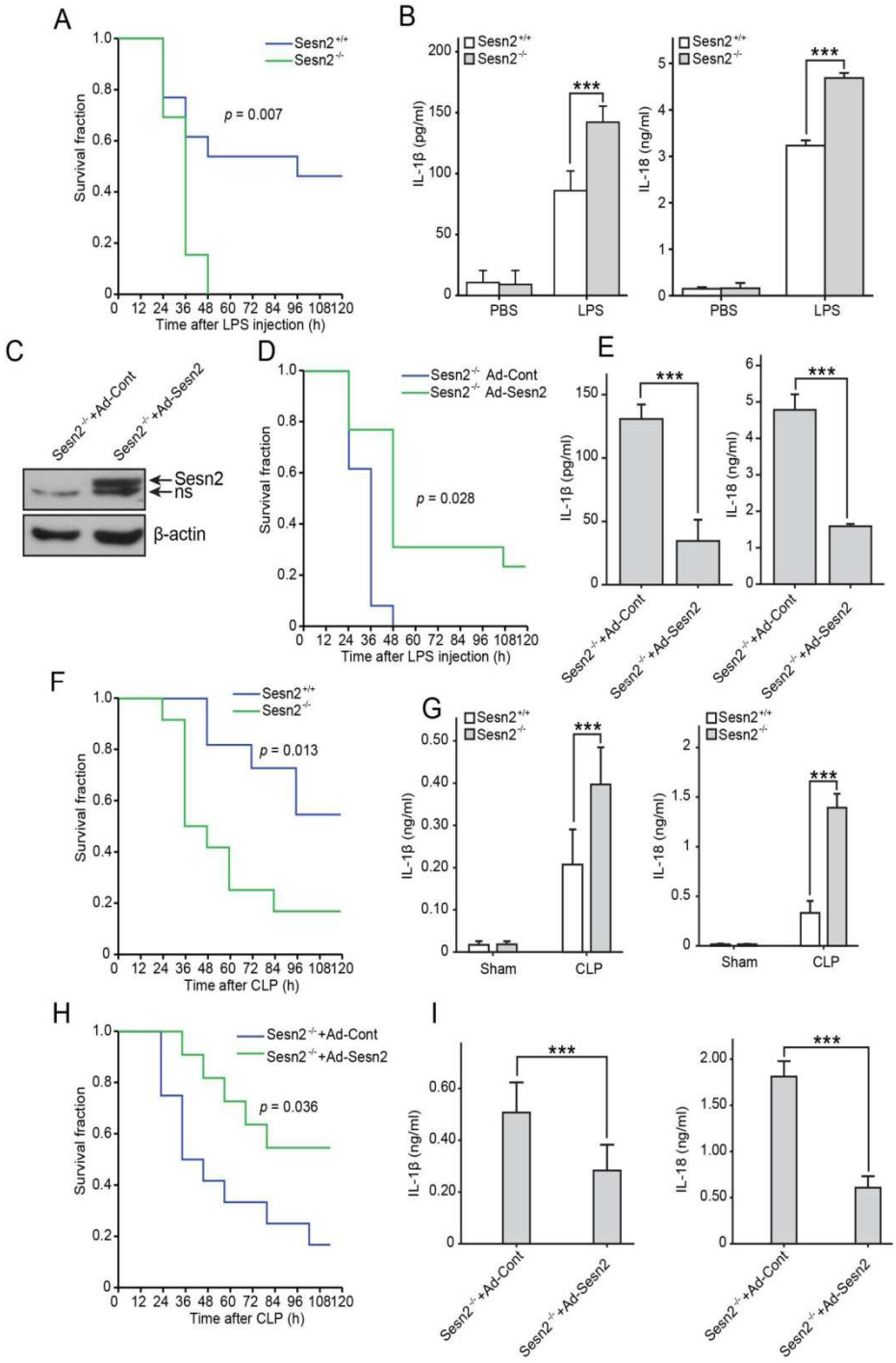
A
Survival fraction
Time after LPS injection (h)
Sesn2+/+
Sesn2-/-
p = 0.007
B
IL-1β (pg/ml)
IL-18 (ng/ml)
PBS
LPS
***
C
Sesn2-/- +Ad-Cont
Sesn2-/- +Ad-Sesn2
Sesn2
ns
β-actin
D
Sesn2-/- Ad-Cont
Sesn2-/- Ad-Sesn2
p = 0.028
E
F
p = 0.013
Time after CLP (h)
G
Sham
CLP
H
Sesn2-/- +Ad-Cont
Sesn2-/- +Ad-Sesn2
p = 0.036
I

Figure 1. Sesn2 serves a protective role against septic shock in sepsis mouse models. (A) Survival of $Sesn2^{+/+}$ (n = 13) mice and $Sesn2^{-/-}$ (n = 13) mice after intraperitoneal injection with LPS (25 mg per kg body weight). (B) Enzyme-linked immunosorbent assay (ELISA) for serum IL-1β and IL-18 at 24 h after LPS challenge (12 mg per kg body weight). (C-E) $Sesn2^{-/-}$ mice were injected intravenously with $5x10^9$ pfu of Ad-Control ($Sesn2^{-/-}$ + Ad-Cont) or Ad-Sesn2 ($Sesn2^{-/-}$ + Ad-Sesn2), and were challenged with LPS 2 days later. Immunoblot for Sesn2 in liver tissues from $Sesn2^{-/-}$ + Ad-Cont or $Sesn2^{-/-}$ + Ad-Sesn2. The 'ns' indicates non-specific band (C). Survival of $Sesn2^{-/-}$ + Ad-Cont (n = 13) or $Sesn2^{-/-}$ + Ad-Sesn2 (n = 13) (D) and ELISA for serum IL-1β and IL-18 in $Sesn2^{-/-}$ + Ad-Cont or $Sesn2^{-/-}$ + Ad-Sesn2 (E). (F) Survival of $Sesn2^{+/+}$ (n = 11) mice and $Sesn2^{-/-}$ (n = 12) mice after sepsis induction by CLP. (G) ELISA for serum IL-1β and IL-18 at 24 h after sepsis induction by CLP. (H-I) $Sesn2^{-/-}$ mice were injected intravenously with $5x10^9$ pfu of Ad-Control ($Sesn2^{-/-}$ + Ad-Cont) or Ad-Sesn2 ($Sesn2^{-/-}$ + Ad-Sesn2), and sepsis was induced by CLP 2 days later. Survival of $Sesn2^{-/-}$ +Ad-Cont (n = 12) or $Sesn2^{-/-}$ +Ad-Sesn2 (n = 11) (H). ELISA for serum IL-1β and IL-18 in $Sesn2^{-/-}$ + Ad-Cont or $Sesn2^{-/-}$ + Ad-Sesn2 (I). Survival rates were analyzed by the Kaplan-Meier method with log-rank test. Data shown are representative of three independent experiments. Error bars are means ± SEM, and *p* values from an unpaired Student's *t* test or an ANOVA followed by Tukey's post hoc test are shown. ***p<0.005

2. Deficiency in Sesn2 enhances inflammasome activation in macrophages

To investigate the role of Sesn2 during inflammasome activation, I isolated bone marrow-derived macrophages (BMDMs) from $Sesn2^{-/-}$ mice, and pretreated the cells with LPS, and then stimulated them with ATP. ATP-driven activation of caspase-1 in LPS-primed macrophages is a conventional model for NALP3 inflammasome activation *in vitro*, which acts through signaling pathways mediated by Toll-like receptor 4 and purinergic receptor P2X7[24,25]. First, I examined the effect of Sesn2 on the activation of caspase-1 in BMDMs. The level of the active, cleaved form of caspase-1 in $Sesn2^{+/+}$ BMDMs increased, reaching its peak at 6 h, and then dramatically decreased at 12 h after treatment with LPS and ATP (Figure 2A). In $Sesn2^{-/-}$ BMDMs, significant amounts of cleaved caspase-1 remained at 12 h after same treatment (Figure 2A). In agreement with the increased cleaved caspase-1 in $Sesn2^{-/-}$, much more of the cleaved form of IL-1β was detected in the supernatant of $Sesn2^{-/-}$ at 12 h after stimulation, compared to $Sesn2^{+/+}$ (Figure 2A). However, the induction level of pro-IL-1β did not differ between $Sesn2^{+/+}$ and $Sesn2^{-/-}$ at any stimulation time point (Figure 2A). Moreover, protein levels of NLRP3 and ASC, components of the NLRP3 complex, and P2X7 were not changed in $Sesn2^{-/-}$ in response to LPS and ATP (Figure 2A). I next examined the secretion level of the caspase-1-dependent cytokines, IL-1β and IL-18, in the supernatant of $Sesn2^{-/-}$ BMDMs. Much higher secretion of IL-1β and IL-18 was detected in $Sesn2^{-/-}$ at 12 h, rather than at 6 h, after stimulation, compared to $Sesn2^{+/+}$ (Figure 2B). I observed that, unlike IL-1β and IL-18 secretion, secretion of tumor necrosis factor-α (TNF-α) was not affected in $Sesn2^{-/-}$ (Figure 2B). The increase of Sesn2 expression started 12 h after treatment with LPS and ATP (Figure 2A). However, the transcription level of Sesn2 was not increased by the same stimulation (data not shown), suggesting that the signal-dependent Sesn2 increase is a result of post-transcriptional regulation of Sesn2 expression. I similarly observed more

IL-1β and IL-18 secretion in peritoneal macrophages derived from Sesn2$^{-/-}$ mice in response to LPS and ATP (Figure 2C). Collectively, these results demonstrate that absence of Sesn2 increases caspase-1 activation and the secretion of IL-1β and IL-18 in macrophages in response to LPS and ATP.

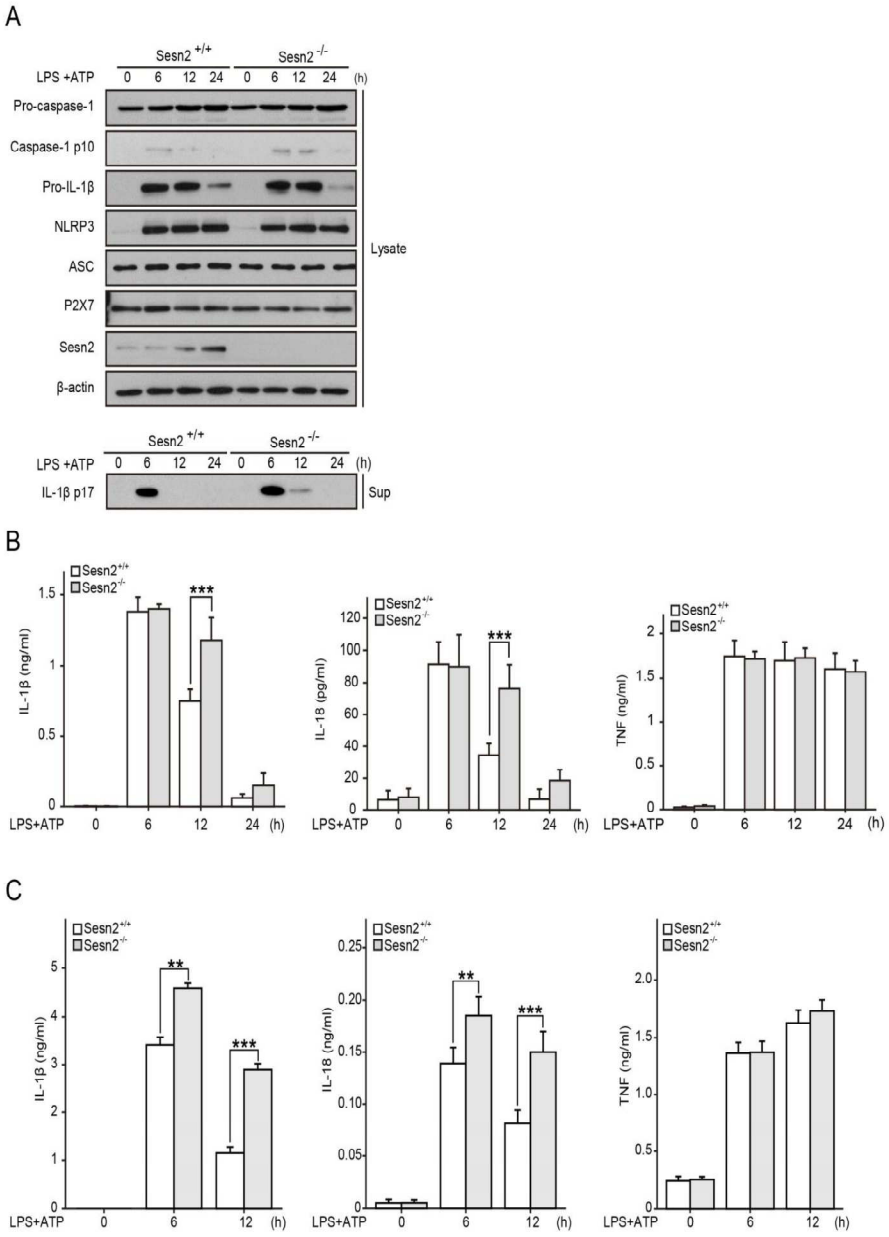
A
Sesn2 +/+
Sesn2 -/-
LPS +ATP
0 6 12 24 0 6 12 24 (h)
Pro-caspase-1
Caspase-1 p10
Pro-IL-1β
NLRP3
ASC
P2X7
Sesn2
β-actin
Lysate
IL-1β p17
Sup
B
Sesn2+/+
Sesn2-/-
IL-1β (ng/ml)
IL-18 (pg/ml)
TNF (ng/ml)
LPS+ATP 0 6 12 24 (h)
***
C
IL-1β (ng/ml)
IL-18 (ng/ml)
TNF (ng/ml)
**
***

Figure 2. Absence in Sesn2 enhances inflammasome activation in macrophages. (A and B) Immunoblots for pro-caspase-1, caspase-1 p10, pro-IL-1β, NLRP3, ASC, P2X7 and Sesn2 in the lysates, and cleaved IL-1β in the supernatants (Sup) (A), and ELISA for IL-1β, IL-18 and TNF in the supernatants (B) of bone marrow-derived macrophages (BMDMs) obtained from $Sesn2^{-/-}$ mice and corresponding wild-type littermate mice ($Sesn2^{+/+}$), then primed with LPS (100ng/ml for 0, 6, 12, 24 h) followed by 30 min of 1mM ATP treatment. (C) ELISA for IL-1β, IL-18 and TNF in the supernatants of peritoneal macrophages obtained from $Sesn2^{-/-}$ or $Sesn2^{+/+}$ mice, then primed with LPS (0, 6, and 12 h) followed by ATP treatment. Data shown are representative of three or more independent experiments. Error bars are means ± SEM, and *p* values from an ANOVA followed by Tukey's post hoc test are shown. ** $p<0.01$, *** $p<0.005$

3. Depletion of Sesn2 impairs mitochondrial homeostasis

Treatment with LPS and ATP produces damaged mitochondria, followed by mitochondrial ROS generation, leading to NLRP3 inflammasome activation in macrophages[11]. I thus hypothesized that Sesn2 might suppress NLRP3 activation through regulation of mitochondrial homeostasis. To test this model, I examined mitochondrial superoxide production at 12 h after stimulation with the use of MitoSOX (a mitochondrial superoxide indicator). Stimulation with LPS and ATP increased the production of mitochondrial superoxide in $Sesn2^{-/-}$ to a greater extent than in $Sesn2^{+/+}$, although there was no difference between mitochondrial ROS production in $Sesn2^{-/-}$ and that in $Sesn2^{-/-}$ at a basal level (Figure 3A). I further analyzed the functional mitochondrial pool in $Sesn2^{-/-}$ through the use of MitoTracker Deep Red, a probe sensitive to the mitochondrial inner transmembrane potential, and MitoTracker Green, a probe for mitochondrial membrane lipids independent of membrane potential. The percentages of damaged mitochondria (positive for MitoTracker Green and negative for MitoTracker Deep Red) following stimulation were 11.7% and 7.1% in $Sesn2^{-/-}$ and $Sesn2^{+/+}$ BMDMs, respectively (Figure 3B). These results revealed an ~1.6-fold greater mitochondrial damage index in $Sesn2^{-/-}$ than in $Sesn2^{+/+}$ (Figure 3B). Given the critical role of Sesn2 in suppression of both mitochondrial damage and hyper-activation of the inflammasome by LPS and ATP, I next investigated the effect of mitochondrial ROS on caspase-1 activation in $Sesn2^{-/-}$. I observed that treatment of Mito-TEMPO, mitochondria-targeted ROS scavenger, abrogates the obvious increase in caspase-1 activation and secretion of IL-1β, but not of TNF-α, in $Sesn2^{-/-}$ (Figures 3C and 3D). These data indicate that Sesn2 suppresses incessant activation of NLRP3 inflammasomes in response to LPS and ATP through maintenance of mitochondrial integrity.

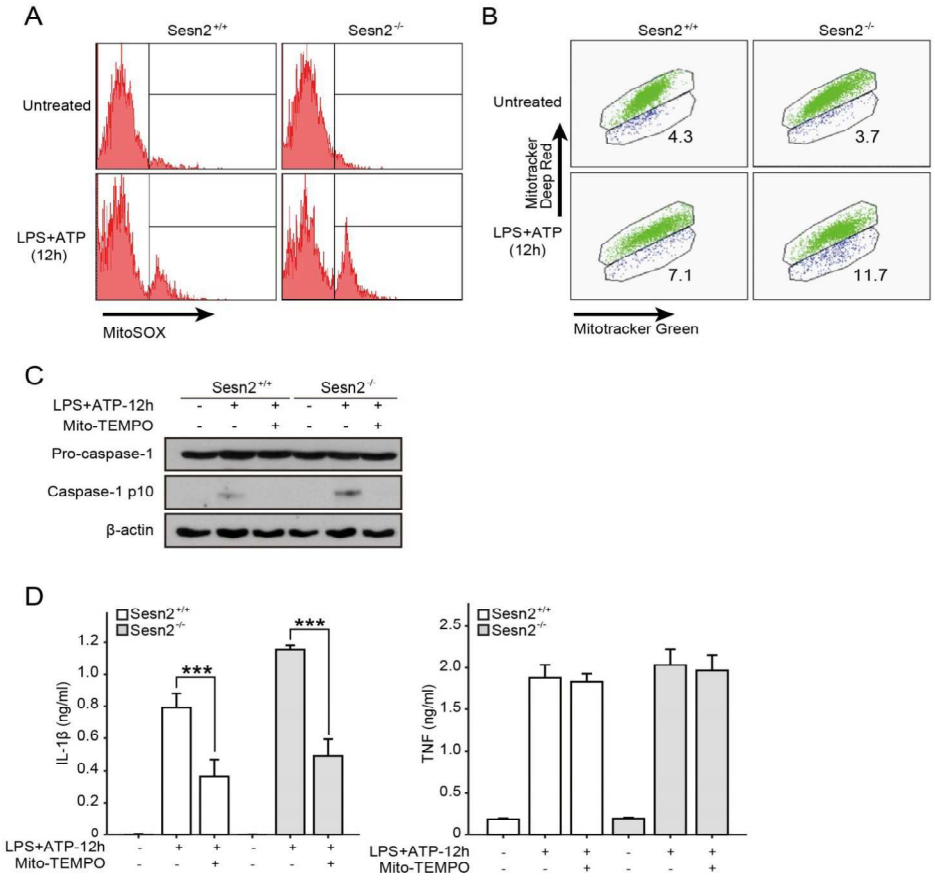

Figure 3. Deficiency of Sesn2 impairs mitochondrial homeostasis. (A and B) Flow cytometry of BMDMs labeled with MitoSOX for 15 min (A) and Flow cytometry of BMDMs stained with MitoTracker Deep Red and MitoTracker Green for 15 min (B) of $Sesn2^{+/+}$ or $Sesn2^{-/-}$ left untreated or primed with LPS for 12 h followed by ATP treatment. (C and D) Immunoblots for pro-caspase-1, caspase-1 p10 (C) and ELISA for IL-1β and TNF in the supernatants (D) in $Sesn2^{+/+}$ or $Sesn2^{-/-}$ BMDMs incubated with Mito-TEMPO (500 μM) for 1 h followed by LPS and ATP treatment. Representative flow cytometry plots are shown. Data shown are representative of three or more independent experiments. Error bars are means ± SEM, and *p* values from an ANOVA followed by Tukey's post hoc test are shown. ***$p<0.005$

4. Sesn2 induces the perinuclear clustering of damaged mitochondria by mediating an aggregation of p62 and its recruitment to Lys 63 ubiquitins on mitochondria surface

I sought to discover the regulatory mechanism whereby Sesn2 prevents the over-production of mitochondrial ROS and aggravation of mitochondrial permeability transition (MPT) generated by damaged mitochondria upon stimulation with LPS and ATP. I first examined whether Sesn2 moves to mitochondria upon stimulation. Sesn2 was translocated into mitochondria at 12 h, rather than 6 h, upon stimulaiton (Figure 4A). I also examined the protein level and translocation of p62 into mitochondria upon stimulation, because Sesn2 acts as a physiologic function through an interaction with p62 in liver tissues or cellular level under oxidative stress condition[18,26]. Although p62 expression began to increase and move into mitochondria at 6 h after stimulation, much more p62 had migrated into mitochondria at 12 h, by which time Sesn2 had been recruited to mitochondria (Figure 4A). To know which protein, of Sesn2 and p62, is responsible for their translocation into mitochondria, I examined Sesn2 and p62 translocation into mitochondria in $p62^{-/-}$ or $Sesn2^{-/-}$, respectively. As shown in Figure 4B, translocation of Sesn2 was decreased in $p62^{-/-}$ upon stimulation, whereas translocation of p62 was not affected in $Sesn2^{-/-}$, indicating that p62 augments Sesn2 translocation into mitochondria, while Sesn2 is not required for p62 translocation into mitochondria. To determine the functional relationships between Sesn2 and p62 for regulation of mitochondrial homeostasis, I compared the mitochondria condition and p62 localization between $Sesn2^{+/+}$ and $Sesn2^{-/-}$. In $Sesn2^{+/+}$, p62 aggregation and perinuclear clustering of mitochondria was observed, and aggregated p62 was colocalized to perinuclear clustered mitochondria upon stimulation (Figure 4C). In contrast, p62 aggregation and perinuclear clustering of mitochondria were rarely detected in $Sesn2^{-/-}$ (Figure 4C). Thus, aggregated p62 was also rarely co-localized to perinuclear clustered

mitochondria in Sesn2$^{-/-}$ (Figure 4C). Given thess findings, I wondered how Sesn2 induces the p62 aggregation and its colocalization on perinuclear clustered mitochondria. Several studies in neuronal cells have shown that perinuclear clustering of mitochondria is initiated when mitochondria are damaged by various cellular stimuli, and is prerequisite for specific removal of impaired mitochondria through mitochondria-dedicated selective autophagy (termed mitophagy)[27,28]. In this context, p62 is required for perinuclear clustering of damaged mitochondria through its aggregation and interaction with ubiquitins on mitochondria surface, because of p62 has a ubiquitin binding domain[29-31]. Thus, I hypothesized that Sesn2 might induce perinuclear clustering of mitochondria by both mediating aggregation of p62 via interaction with p62 and linking p62 to ubiquitins on damaged mitochondria surface. As expected, endogenous Sesn2 interacted with p62 at 12 h after stimulation with LPS and ATP (Figure 4D). I examined the spatial proximity of p62 to Lys (K)63- or K48-linked ubiquitins on mitochondria following stimulation by *in situ* proximity-ligation assay (a method that permits visualization of the spatial proximity of two proteins). p62 recruitment to K63-linked ubiquitins, but not K48-linked ubiquitins, on perinuclear-clustered mitochondria, was observed in Sesn2$^{+/+}$, while p62 recruitment to K63-linked ubiquitins was rarely detected in Sesn2$^{-/-}$ (Figure 4E). Collectively, Sesn2 facilitates the perinuclear clustering of damaged mitochondria by mediating an aggregation of p62 and its recruitment to K63-linked ubiquitins on mitochondria surface.

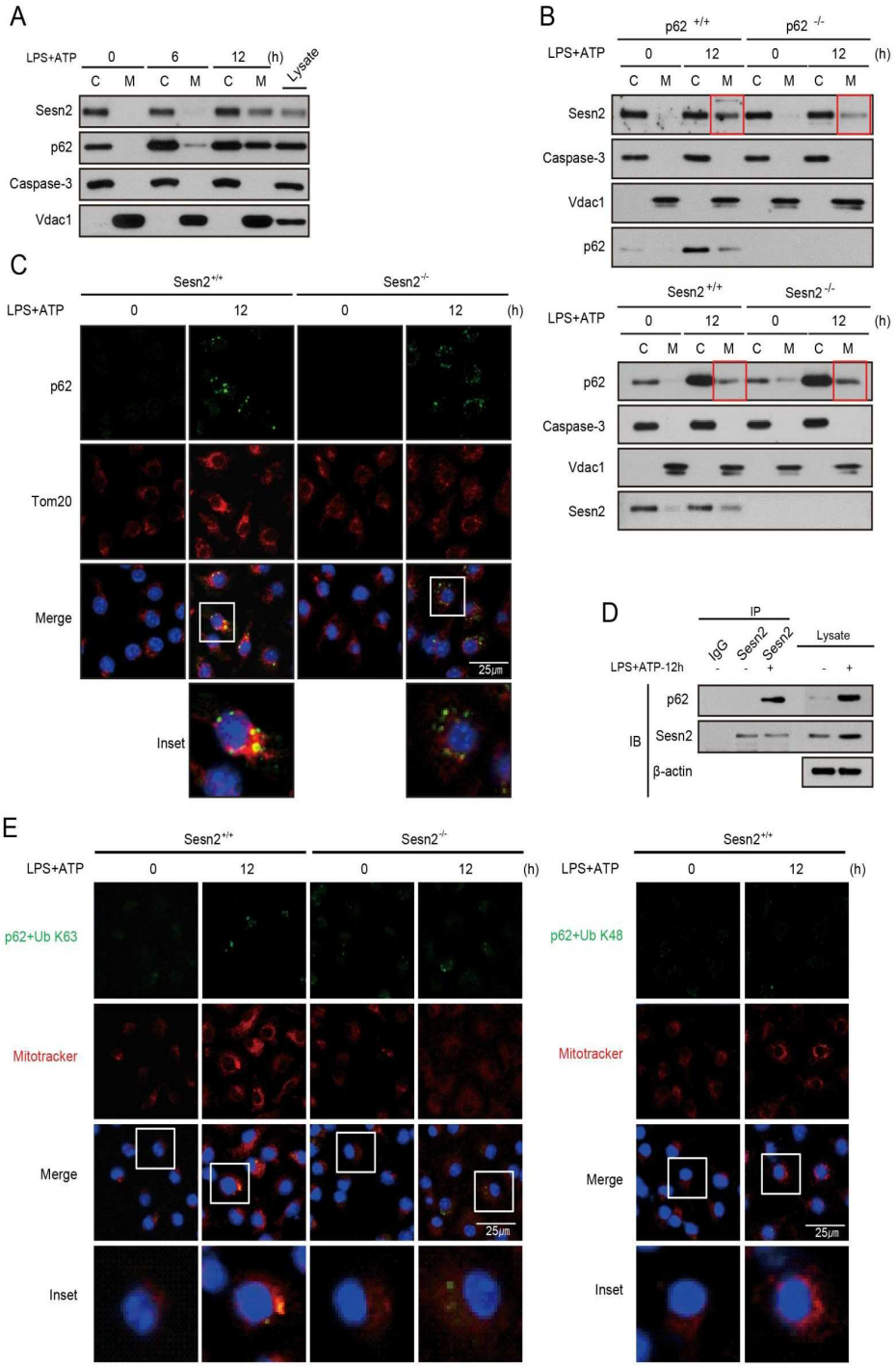
A
LPS+ATP
0
6
12
(h)
C
M
Lysate
Sesn2
p62
Caspase-3
Vdac1
B
p62 +/+
p62 -/-
Caspase-3
Vdac1
C
Sesn2+/+
Sesn2-/-
Tom20
Merge
Inset
25μm
D
IP
IgG
Sesn2
Lysate
LPS+ATP-12h
IB
β-actin
E
p62+Ub K63
Mitotracker
p62+Ub K48

Figure 4. Sesn2 induces the perinuclear clustering of damaged mitochondria in response to LPS and ATP. (A) Subcellular fractionation of Wild-type (WT) BMDMs. BMDMs were primed with LPS (0, 6, 12 h) followed by ATP treatment. Mitochondrial (M) and cytosolic (C) fractions were obtained and analyzed for expression of Sesn2 and p62 by immunoblot. Purity of the fractions was assessed by blotting for Vdac1 (mitochondrial protein) and Caspase3 (cytosolic protein). (B) Subcellular fractionation of $p62^{+/+}$ and $p62^{-/-}$ or $Sesn2^{+/+}$ and $Sesn2^{-/-}$ BMDMs. BMDMs were primed with LPS for 12h followed by ATP treatment, and mitochondrial (M) and cytosolic (C) fractions were obtained and analyzed for expression of Sesn2 and p62 by immunoblot. (C) Representative confocal immunofluorescence images of p62 colocalizing with Tom20 (mitochondria surface membrane protein) in $Sesn2^{+/+}$ or $Sesn2^{-/-}$ BMDMs primed with LPS for 12 h followed by ATP treatment. (D) Immunoblots of Sesn2 immunoprecipitates (IP: left) and total lysates (right) of WT BMDMs primed with LPS for 12 h followed by ATP treatment, probed for p62 and Sesn2. (E) Proximity-ligation assay of p62 and K63 or K48 ubiquitin, and their colocalization with Mitotracker in $Sesn2^{+/+}$ and $Sesn2^{-/-}$ BMDMs primed with LPS for 12 h followed by ATP treatment. Imaging data are representative of several images from three independent experiments. Data shown are representative of three or more independent experiments.

5. p62 suppresses continuous activation of inflammasomes through maintenance of mitochondrial integrity and protects against septic shock condition

To test whether p62 itself is critical for perinuclear clustering of mitochondria, I examined the levels of clustered mitochondria in $p62^{-/-}$ BMDMs in response to LPS and ATP. Large numbers of perinuclear clustered mitochondria were observed in $p62^{+/+}$, while perinuclear clustered mitochondria were not detected in $p62^{-/-}$ (Figure 5A). Stimulation with LPS and ATP increased the production of mitochondrial ROS in $p62^{-/-}$ to a greater amount than in $p62^{+/+}$ (Figure 5B). The percentages of damaged mitochondria were more increased in $p62^{-/-}$ than $p62^{+/+}$ (Figure 5C). I also examined the role of p62 in inflammasome activation by LPS and ATP. More of the cleaved form of caspase-1, and secretion of IL-1β and IL-18 were detected in $p62^{-/-}$ than in $p62^{+/+}$ (Figures 5D and 5E). I tested whether the inhibitory role of p62 in inflammasome activation could be adapted to an *in vivo* septic shock model. Serum concentrations of IL-1β and IL-18 were higher in endotoxemic $p62^{-/-}$ than in $p62^{+/+}$ (Figure 6A). $p62^{-/-}$ had significantly higher mortality rates than did $p62^{+/+}$ mice (Figure 6B). I also examined the rescue effect of p62 through intravenous infection with an adenoviral vector containing the human p62 gene (Ad-p62) into $p62^{-/-}$ mice. I verified that p62 expression in liver was detectable following injection with Ad-p62, but not Ad-Cont (Figure 6C). Serum concentrations of IL-1β and IL-18 were decreased by rescue with Ad-p62 in endotoxemia $p62^{-/-}$ (Figure 6D). These results indicate that, similar to Sesn2, p62 not only prohibits incessant inflammasome activation via maintenance of mitochondrial homeostasis, but also protects against septic shock condition.

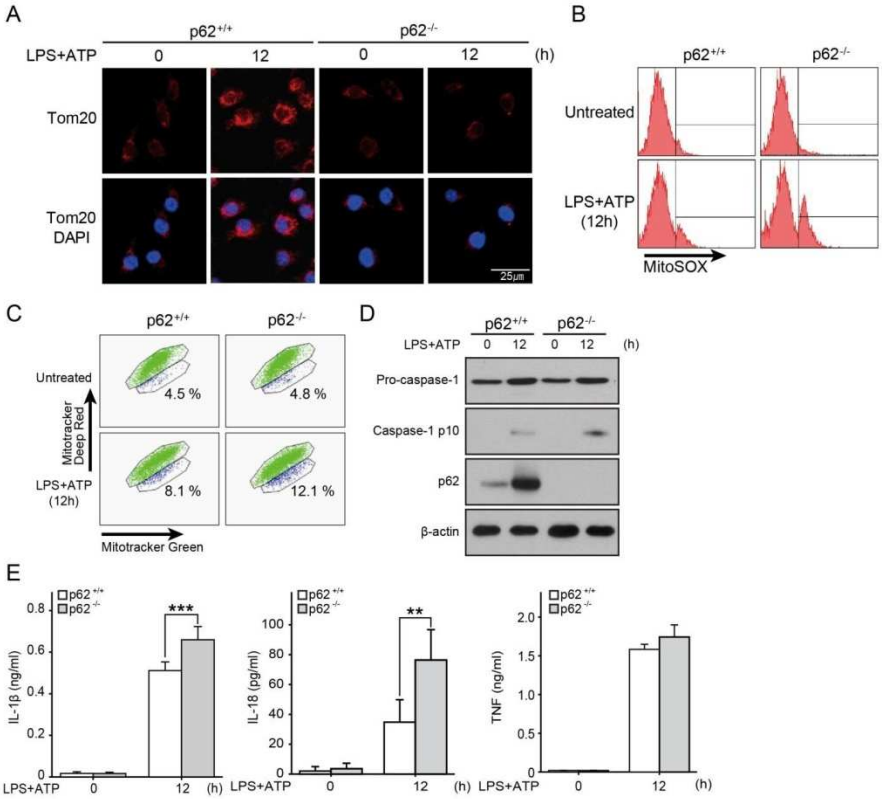

Figure 5. p62 suppresses continuous activation of inflammasomes through maintenance of mitochondrial integrity (A-E) $p62^{+/+}$ or $p62^{-/-}$ BMDMs were primed with LPS for 12 h followed by ATP treatment. Representative confocal immunofluorescence images of perinuclear clustered mitochondria by Tom20 staining (A), Flow cytometry of BMDMs labeled for 15 min with MitoSOX (B), Flow cytometry of BMDMs stained for 15 min with MitoTracker Deep Red and MitoTracker Green (C), Immunoblots of pro-caspase-1, caspase-1 p10 and p62 (D), ELISA for IL-1β, IL-18 and TNF in the supernatants (E). Imaging data are representative of several images from two independent experiments. Representative flow cytometry plots are represented. Data shown are representative of three or more independent experiments. Error bars are means ± SEM, and *p* values from an unpaired Student's *t* test or an ANOVA followed by Tukey's post hoc test are shown. ** $p<0.01$, *** $p<0.005$

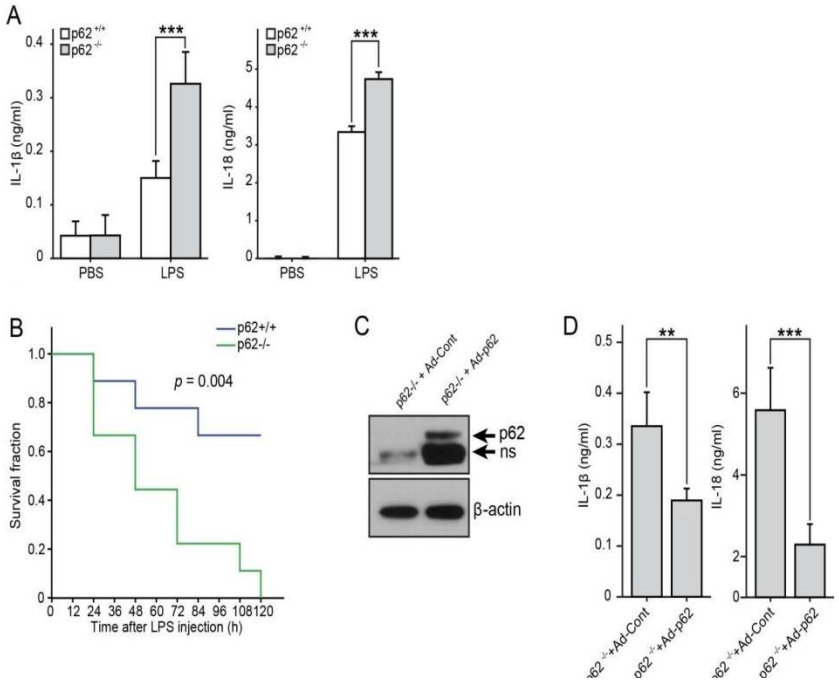

Figure 6. p62 protects against septic shock condition. (A and B) $p62^{+/+}$ or $p62^{-/-}$ mice were intraperitoneally injected with LPS. ELISA for serum IL-1β and IL-18 at 24 h after LPS challenge (12 mg per kg body weight) (A) and Survival of $p62^{+/+}$ (n = 9) mice and $p62^{-/-}$ (n = 9) mice after intraperitoneal injection of LPS (25 mg per kg body weight) (B). (C-D) $p62^{-/-}$ mice were injected intravenously with $5x10^9$ pfu of Ad-Control ($p62^{-/-}$ + Ad-Cont) or Ad-p62 ($p62^{-/-}$ + Ad-p62), and were challenged with LPS 2 days later. Immunoblot for p62 in liver tissues from $p62^{-/-}$ + Ad-Cont or $p62^{-/-}$ + Ad-p62 mice. 'ns' indicates non-specific band (C) and ELISA for serum IL-1β and IL-18 in $p62^{-/-}$ mice + Ad-Cont or + Ad-p62 (D). The survival rate was analyzed by the Kaplan-Meier method with log-rank test. Data shown are representative of three or more independent experiments. Error bars are means ± SEM, and *p* values from an unpaired Student's *t* test or an ANOVA followed by Tukey's post hoc test are shown. ** $p<0.01$, *** $p<0.005$

6. Sesn2 induces autophagosome formation and consequent mitophagy

I hypothesized that, in addition to the critical role of Sesn2 in induction of perinuclear clustering of damaged mitochondria, it might also activate selective autophagy to remove perinuclear clustered mitochondria in response to LPS and ATP. I first checked the level of autophagosome formation by assaying for the GFP-LC3-II form and GFP fragments generated by the degradation of GFP-LC3 inside autolysosomes in GFP-LC3 transgenic mice in a $Sesn2^{+/+}$ ($Sesn2^{+/+}$/GFP-LC3) or $Sesn2^{-/-}$ ($Sesn2^{-/-}$/GFP-LC3) genetic background. At 12 h, rather than 6 h, after stimulation with LPS and ATP, the GFP-LC3-II form and GFP fragments were detectable at lower levels in $Sesn2^{-/-}$/GFP-LC3 than in $Sesn2^{+/+}$/GFP-LC3 (Figure 7A). In the presence of bafilomycin A1, which inhibits the degradation of autophagosomes, endogenous LC3-II forms were decreased in $Sesn2^{-/-}$ (Figure 7B). In addition, I determined the number of cells with more than three strong GFP-LC3 puncta among the total cells in $Sesn2^{+/+}$/GFP-LC3 and $Sesn2^{-/-}$/GFP-LC3 following stimulation with LPS and ATP. The number of cells with GFP-LC3 puncta was lower in $Sesn2^{-/-}$/GFP-LC3 than in $Sesn2^{+/+}$/GFP-LC3 (Figures 7C and 7D), indicating that Sesn2 itself induces autophagosome formation at 12 h after stimulation with LPS and ATP. I next investigated whether Sesn2 is involved in mitophagy by analyzing the number of cells that colocalize GFP-LC3 puncta with perinuclear clustered mitochondria among cells with GFP-LC3 puncta. The number of colocalezed cells was lower in $Sesn2^{-/-}$/GFP-LC3 than in $Sesn2^{+/+}$/GFP-LC3 (Figures 7C and 7E). Furthermore, damaged mitochondria surrounded by autolysosomes were detected in the perinuclear region of $Sesn2^{+/+}$ following stimulation, while a greater abundance of swollen mitochondria with severely disrupted cristae were observed throughout the cytoplasm of $Sesn2^{-/-}$ (Figure 7F). I wondered how Sesn2 induces autophagosome formation and mitophagy upon stimulation. It is known that AMP-activated protein kinase (AMPK) and

mammalian target of rapamycin complex 1 (mTORC1) are closely involved in initiation of autophagy in response to nutrient signaling[32-34], and Sesn2 has been reported to regulate the activity of AMPK and mTORC1 in response to genotoxic stress[35]. Thus, I examined whether Sesn2 regulates the activity of AMPK and mTORC1 upon stimulation with LPS and ATP. The extent of phosphorylation of AMPK-α, SP6, and Acetyl-CoA carboxylase (ACC) was not affected in $Sesn2^{-/-}$, compared to that in $Sesn2^{+/+}$ (Figure 7G), indicating that Sesn2 is not involved in activation of the AMPK or mTOR signaling pathways in response to LPS and ATP in macrophages.

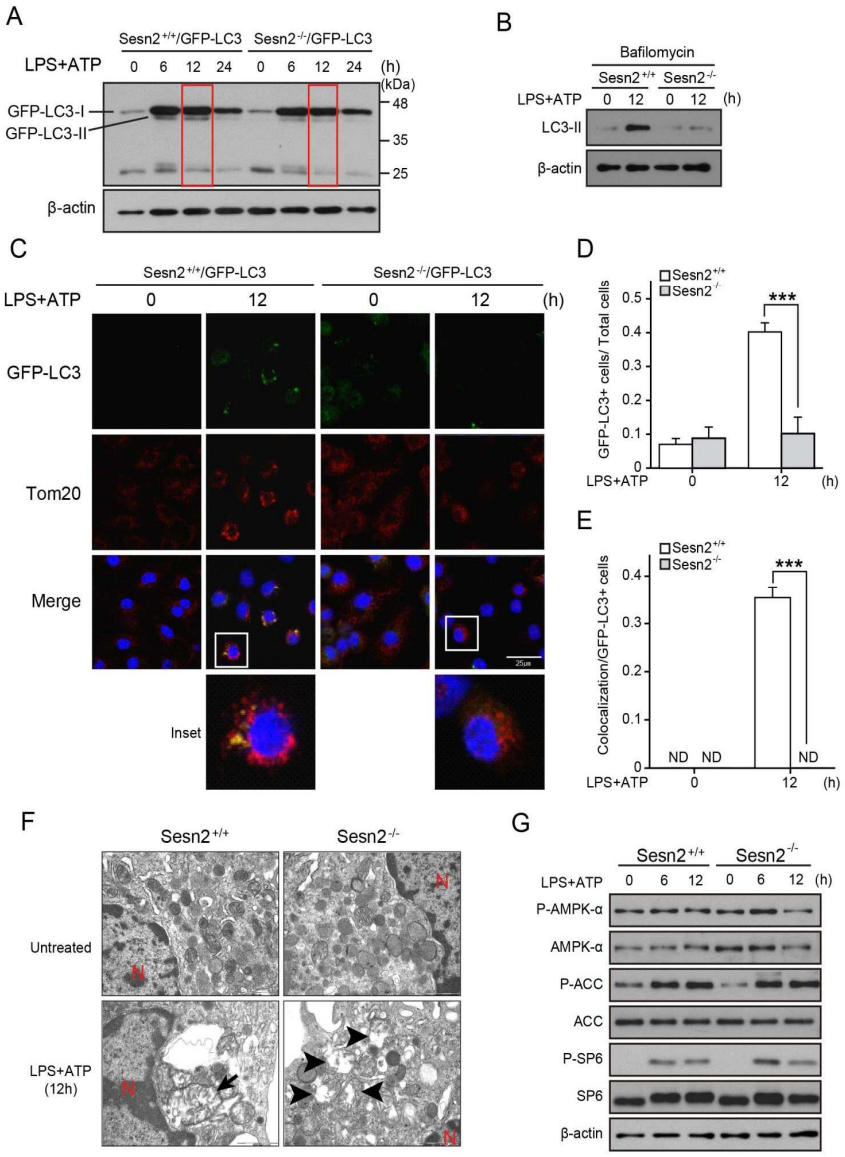
A
Sesn2+/+/GFP-LC3
Sesn2-/-/GFP-LC3
LPS+ATP
0 6 12 24 0 6 12 24 (h)
(kDa)
GFP-LC3-I
GFP-LC3-II
48
35
25
β-actin
B
Bafilomycin
Sesn2+/+
Sesn2-/-
LPS+ATP
0 12 0 12 (h)
LC3-II
β-actin
C
Sesn2+/+/GFP-LC3
Sesn2-/-/GFP-LC3
LPS+ATP
0 12 0 12 (h)
GFP-LC3
Tom20
Merge
Inset
25μm
D
Sesn2+/+
Sesn2-/-
GFP-LC3+ cells/ Total cells
0.5
0.4
0.3
0.2
0.1
0
***
LPS+ATP
0 12 (h)
E
Sesn2+/+
Sesn2-/-
Colocalization/GFP-LC3+ cells
0.4
0.3
0.2
0.1
0
***
ND ND ND
LPS+ATP
0 12 (h)
F
Sesn2+/+
Sesn2-/-
Untreated
LPS+ATP
(12h)
N
G
Sesn2+/+
Sesn2-/-
LPS+ATP
0 6 12 0 6 12 (h)
P-AMPK-α
AMPK-α
P-ACC
ACC
P-SP6
SP6
β-actin

Figure 7. Sesn2 induces autophagosome formation and consequent mitophagy (A) Immunoblot with an anti-GFP antibody in BMDMs obtained from GFP-LC3 transgenic mice with a $Sesn2^{+/+}$ ($Sesn2^{+/+}$/GFP-LC3) or $Sesn2^{-/-}$ ($Sesn2^{-/-}$/GFP-LC3) genetic background. BMDMs were primed with LPS (0, 6, 12, 24 h) followed by 30 min of ATP treatment. (B) Immunoblot for LC3-II in $Sesn2^{+/+}$ or $Sesn2^{-/-}$ BMDMs primed with LPS for 12h followed by ATP in the presence of bafilomycin. (C-E) Representative confocal immunofluorescence images of GFP-LC3 colocalizing with Tom20 (C), Quantification of number of cells with more than three strong GFP-LC3 puncta among total cells (D), Quantification of number of cells with more than three strong GFP-LC3 puncta colocalizing with perinuclear clustered mitochondria among cells with more than three strong GFP-LC3 puncta (E) in $Sesn2^{+/+}$/GFP-LC3 and $Sesn2^{-/-}$/GFP-LC3 BMDMs primed with LPS for 12 h followed by ATP treatment. (F) Transmission electron microscopy of morphological changes in mitochondria in $Sesn2^{+/+}$ or $Sesn2^{-/-}$ BMDMs primed with LPS for 12 h followed by ATP treatment. (arrow, mitochondria within autophagosomes; arrowhead, damaged mitocondria; red 'N', nucleus). (G) Immunoblots for AMPKα, phospho-AMPKα (P-AMPK), ACC, phospho-ACC (P-ACC), SP6 and phospho-SP6 (P-SP6) in $Sesn2^{+/+}$ or $Sesn2^{-/-}$ BMDMs primed with LPS (0, 6, 12 h) followed by ATP treatment. Imaging data are representative of several images from two or more independent experiments. Data shown are representative of three or more independent experiments. Error bars are means ± SEM, and *p* values from an ANOVA followed by Tukey's post hoc test are shown. ***$p<0.005$. ND; not detectable.

7. Sesn2 induces mitophagy via maintenance of ULK1 protein stability

I next investigated whether Sesn2 regulates expression of various autophagy-related proteins that are known to initiate or activate autophagy. Surprisingly, the increase in ULK1 (UNC-51-like kinase 1, the mammalian ortholog of yeast Atg1) at 12 h after stimulation with LPS and ATP was significantly lower in $Sesn2^{-/-}$, while expression levels of other ATG-related proteins, including beclin1, Atg5, Atg7, and ULK2 were not changed in $Sesn2^{-/-}$ (Figure 8A). Same as Sesn2, ULK1 was translocated into mitochondria at 12 h upon stimulation (Figure 8B). To verify that defective autophagosome formation in $Sesn2^{-/-}$ is attributable to a decrease of ULK1, I examined the rescue effect of Sesn2 deficiency through injection of human ULK1 expressed virus particles into $Sesn2^{-/-}$ BMDMs. I identified ULK1 expression in $Sesn2^{-/-}$ (Figure 8C). Rescue with ULK1 increased the number of cells with GFP-LC3 puncta, but did not rescue the perinuclear clustering of mitochondria (Figures 8D and 8E). Both mitochondrial ROS and damaged mitochondria were decreased by rescue with ULK1 (Figures 9A and 9B). In accordance with the results on mitochondrial homeostasis, cleaved caspase-1 and secretion of IL-1β and IL-18 were decreased by rescue with ULK1 (Figures 9C and 9D). These results indicate that Sesn2 functions as an upstream regulator of ULK1 in autophagosome formation and mitophagy via maintenance of ULK1 protein stability.

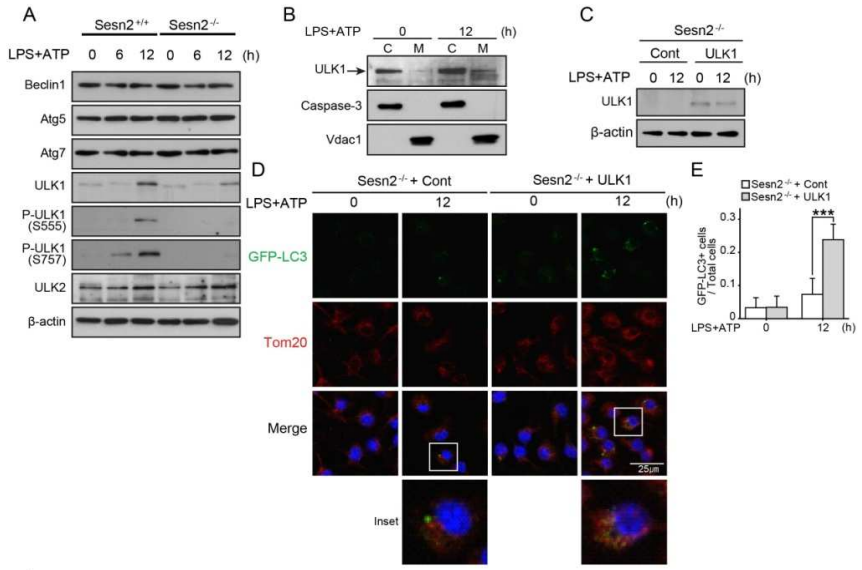

Figure 8. Sesn2 induces mitophagy via maintenance of ULK1 protein stability. (A) Immunoblots for Beclin1, Atg5, Atg7, ULK1, phospho-ULK1 (P-ULK1 S555 and P-ULK1 S757), and ULK2 in Sesn2$^{+/+}$ or Sesn2$^{-/-}$ BMDMs primed with LPS (0, 6, 12 h) followed by ATP treatment. (B) Subcellular fractionation of Wild-type (WT) BMDMs. BMDMs were primed with LPS (0, 6, 12 h) followed by ATP treatment. Mitochondrial (M) and cytosolic (C) fractions were obtained and analyzed for expression of ULK1 by immunoblot. (C-E) Sesn2$^{-/-}$ BMDMs were infected with retroviral control vector, or retrovirally-mediated human ULK1 expression vector, (Sesn2$^{-/-}$ + Cont, Sesn2$^{-/-}$ + ULK1, respectively), and primed with LPS for 12 h followed by ATP treatment. Immunoblot for ULK1 (C), Representative confocal immunofluorescence images of GFP-LC3 colocalizing with Tom20 (D), Quantification of number of cells with more than three strong GFP-LC3 puncta among total cells (E). Imaging data are representative of several images from two independent experiments. Data shown are representative of three or more independent experiments. Error bars are means ± SEM, and *p* values from an ANOVA followed by Tukey's post hoc test are shown. ***p<0.005

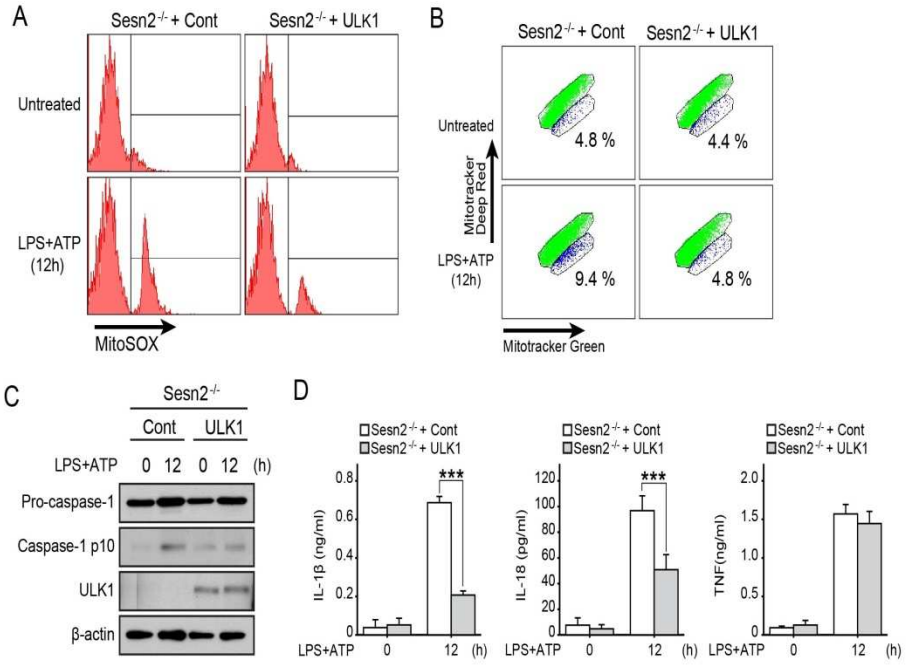

Figure 9. ULK1 suppresses continuous activation of inflammasomes through maintenance of mitochondrial integrity. (A-D) Sesn2$^{-/-}$ BMDMs were infected with retroviral control vector, or retrovirally-mediated human ULK1 expression vector, (Sesn2$^{-/-}$ + Cont, Sesn2$^{-/-}$ + ULK1, respectively), and primed with LPS for 12 h followed by ATP treatment. Flow cytometry of BMDMs labeled for 15 min with MitoSOX (A), Flow cytometry of BMDMs stained for 15 min with MitoTracker Deep Red and MitoTracker Green (B), Immunoblots for pro-caspase-1 and cleaved caspase-1 (C), ELISA for IL-1β, IL-18 and TNF in the supernatants (D). Representative flow cytometry plots are shown. Data shown are representative of three or more independent experiments. Error bars are means ± SEM, and *p* values from an ANOVA followed by Tukey's post hoc test are shown. ***p<0.005

8. p62 is responsible for autophagosome formation and consequent mitophagy

I wondered whether p62 could regulate ULK1 stabilization as Sesn2 did, given that p62, together with Sesn2, is required for maintenance of mitochondrial homeostasis in my study. Neither the increase in ULK1, nor its phosphorylation upon stimulation, were affected in $p62^{-/-}$ (Figure 10A), indicating that p62 is not required for ULK1 stabilization or activation. In addition to the essential role of p62 for perinuclear clustering of damaged mitochondria, I wondered whether p62 itself also could activate specific autophagy to eliminate damaged mitochondria in response to LPS and ATP. In the presence of bafilomycin A1, endogenous LC3-II forms were observed at lower levels in $p62^{-/-}$ than in $p62^{+/+}$ (Figure 10B). Moreover, the number of cells with GFP-LC3 puncta and cells that colocalized GFP-LC3 puncta with perinuclear clustered mitochondria was decreased in $p62^{-/-}$ (Figures 10C-E). Furthermore, damaged mitochondria surrounded by autolysosomes were detected in the perinuclear region of $p62^{+/+}$, while a greater abundance of swollen mitochondria with severely disrupted cristae were observed in the cytoplasm of $p62^{-/-}$ (Figure 10F). Taken together, these findings indicate that p62 mediates the induction of autophagosome formation and consequent mitophagy upon stimulation, but these are not mediated by its regulation of ULK1 activation.

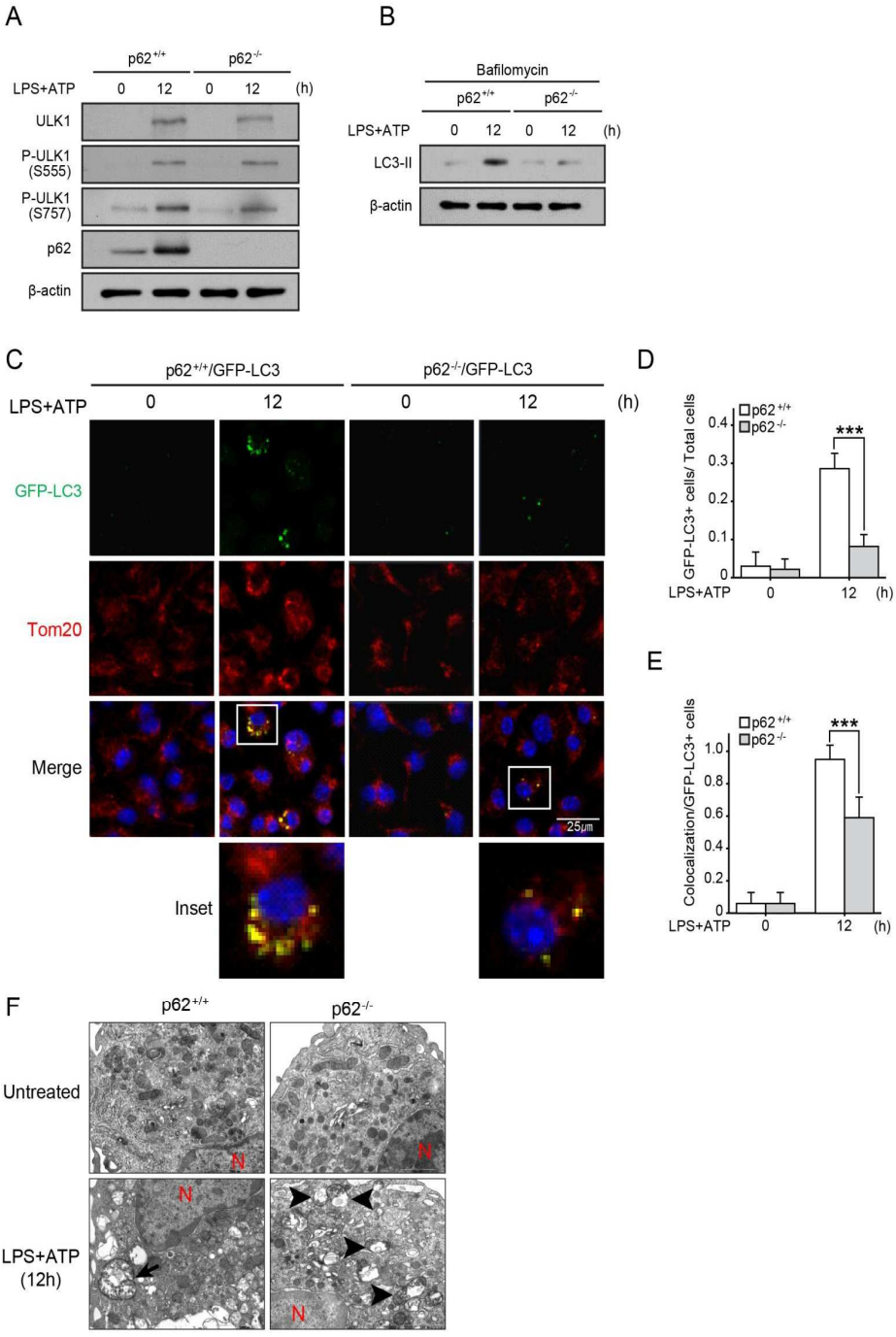
A
p62+/+
p62-/-
LPS+ATP
0
12
0
12
(h)
ULK1
P-ULK1 (S555)
P-ULK1 (S757)
p62
β-actin
B
Bafilomycin
p62+/+
p62-/-
LPS+ATP
0
12
0
12
(h)
LC3-II
β-actin
C
p62+/+/GFP-LC3
p62-/-/GFP-LC3
LPS+ATP
0
12
0
12
(h)
GFP-LC3
Tom20
Merge
25μm
Inset
D
p62+/+
p62-/-
GFP-LC3+ cells/ Total cells
0.4
0.3
0.2
0.1
0
***
LPS+ATP
0
12
(h)
E
p62+/+
p62-/-
Colocalization/GFP-LC3+ cells
1.0
0.8
0.6
0.4
0.2
0
***
LPS+ATP
0
12
(h)
F
p62+/+
p62-/-
Untreated
LPS+ATP (12h)
N
N
N
N

Figure 10. p62 is responsible for autophagosome formation and consequent mitophagy. (A) Immunoblots for ULK1, phospho-ULK1 (S555), and phospho-ULK1 (S757) in $p62^{+/+}$ or $p62^{-/-}$ BMDMs primed with LPS for 12h followed by ATP treatment. (B) Immunoblot for LC3-II in $p62^{+/+}$ or $p62^{-/-}$ BMDMs primed with LPS for 12h followed by ATP treatment in the presence of bafilomycin. (C-E) $p62^{+/+}$ or $p62^{-/-}$ BMDMs were infected with retrovirally-mediated rat GFP-LC3 expression vector, and primed with LPS for 12 h followed by ATP treatment. Representative confocal immunofluorescence images of GFP-LC3 colocalizing with Tom20 (C), Quantification of number of cells with more than three strong GFP-LC3 puncta among total cells (D), Quantification of number of cells with more than three strong GFP-LC3 puncta colocalizing with perinuclear clustered mitochondria among cells with more than three strong GFP-LC3 puncta (E). (F) Transmission electron microscopy of morphological changes in mitochondria in $p62^{+/+}$ or $p62^{-/-}$ BMDMs primed with LPS for 12 h followed by ATP treatment. (arrow, mitochondria within autophagosomes; arrowhead, damaged mitocondria; red 'N', nucleus). Imaging data are representative of several images from three independent experiments. Data shown are representative of three or more independent experiments. Error bars are means ± SEM, and *p* values from an ANOVA followed by Tukey's post hoc test are shown. ***$p<0.005$

9. Protein levels of Sesn2 and ULK1 were increased by mitochondrial ROS generated from damaged mitochondria

I wondered how protein level of Sesn2 and ULK1 are maintained after stimulation of LPS and ATP, because protein expression of Sesn2 and ULK1 were increased at 12 h upon stimulation without increase of mRNA level of them by the same stimulation. I supposed that mitochondrial ROS generated from damaged mitochondria generated by stimulation with LPS and ATP might responsible for protein increase of Sesn2 and ULK1. To probe this, I examined the protein level of Sesn2 and ULK1 at 12 h after stimulation of LPS and ATP in the presence of Mito-TEMPO, mitochondria-targeted ROS scavenger. Removal of mitochondrial ROS decreased the protein level of Sesn2 and ULK1 increased by stimulation (Figure 11). However, protein level of p62 was not decreased by Mito-TEMPO (Figure 11). Given that both mRNA and protein level of p62 were increased at 6 h after stimulation, unlike Sesn2 and ULK1, increase of p62 in mRNA and protein level by stimulation might be regulated by other signaling pathway which is different from mitochondrial ROS-mediated regulation.

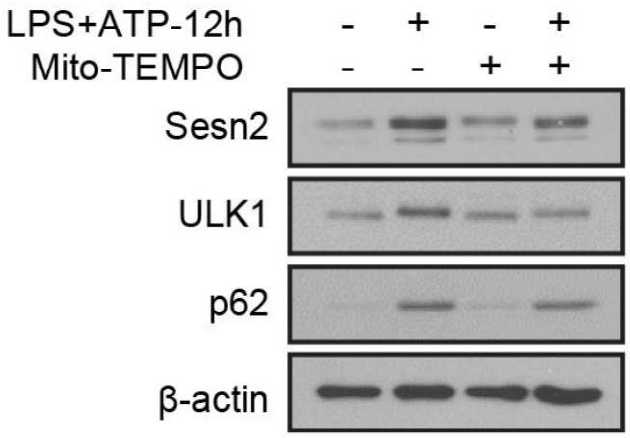

Figure 11. Protein levels of Sesn2 and ULK1 were increased by mitochondrial ROS generated from damaged mitochondria**.** Immunoblots for Sesn2, ULK1 and p62 in WT BMDMs incubated with Mito-TEMPO (500 μM) for 1 h followed by LPS and ATP treatment. Data shown are representative of three or more independent experiments.

10. Human Sesn2 is highly expressed in monocytes of septic shock patients

To verify whether my findings obtained at the cellular level and the organism level in the sepsis mouse model are relevant to human patients with septic shock syndrome, I first measured the secretion levels of IL-1β and IL-18 in the serum of septic patients in the medical intensive care unit (ICU). Similar to the mouse sepsis model, much higher secretion of IL-1β and IL-18 was observed in the serum of septic shock patients than of healthy humans (Figure 12A). More damaged mitochondria were also detected in monocytes isolated from patient blood (Figures 12B and 12C). In this context, I wondered whether the protein level of human Sesn2 or ULK1 is altered in septic shock patients. Interestingly, Sesn2 protein were significantly increased in monocytes of nearly all septic shock patients, compared to health humans in my study (Figure 12D). However, ULK1 were not detected in same experimental condition. In accordance with my cellular data that protein level of Sesn2 was increased by mitochondrial ROS generated by inflammasome stimulators, increase of Sesn2 in septic shock patients might be caused by mitochondrial ROS generated from damaged mitochondria under septic shock conditions. Thus, Sesn2 might play a protective role for resolution in severe inflammatory condition through removal of damaged mitochondria.

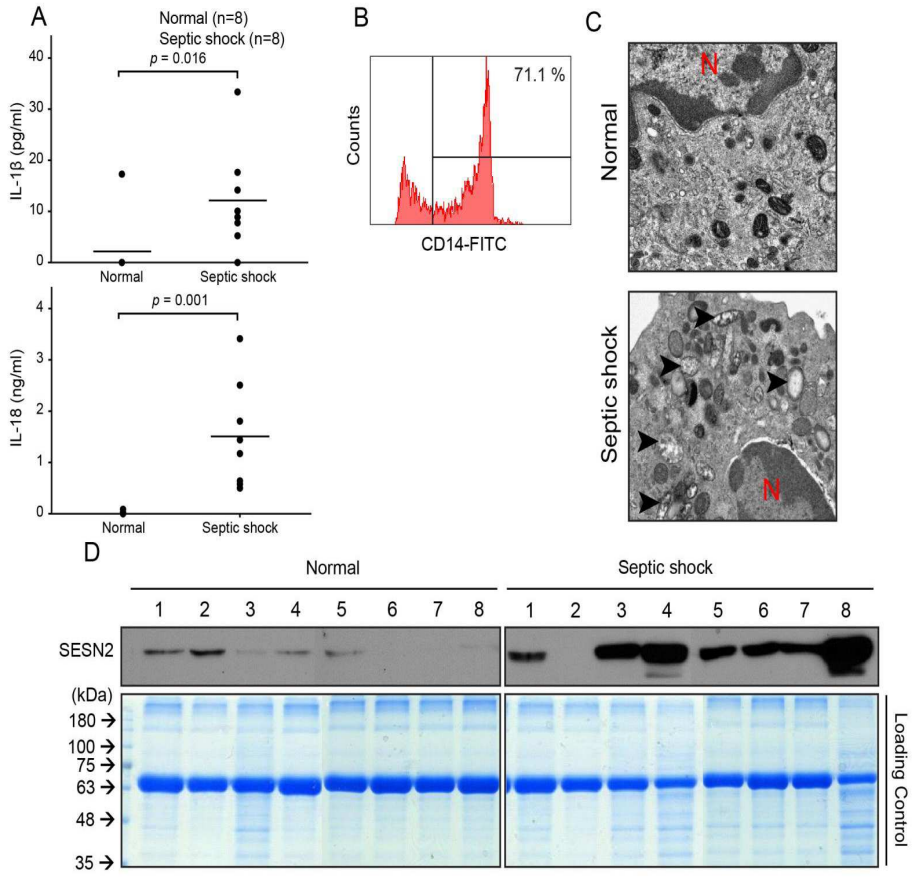

Figure 12. Human Sesn2 is highly expressed in monocytes of septic shock patients. (A-D) Human blood samples were collected from healthy volunteers and septic shock patients. ELISA for IL-1β and IL-18 in plasma (A), Flow cytometry of isolated human monocytes from blood to check the purity with anti-CD14-FITC (B), Transmission electron microscopy of morphological changes in mitochondria in human monocytes isolated from blood (arrowhead, damaged mitochondria; red 'N', nucleus) (C), Immunoblot for SESN2 in isolated human monocytes and Coomassie staining as loading control (D). Imaging data are representative of several images. Representative flow cytometry plots are shown. Data shown are representative of three or more independent experiments. *p* values from an unpaired Student's *t* test.

IV. DISCUSSION

The *in vivo* relevance of Sesn2-mediated signaling to metabolic processes and related diseases has been recently demonstrated[18,21,22,36]. However, the role of Sesn2 in the immune response and the mechanisms concerned *in vivo* has been largely unknown. In addition, the involvement of Sesn2 in regulation of mitochondrial homeostasis has not been explored in detail. I presented a novel role for Sesn2 in the suppression of incessant NLRP3-mediated inflammation by preserving mitochondrial integrity via mitophagy induction. Although published reports have illustrated a critical role for autophagy and mitochondrial homeostasis in regulation of inflammasome activation[11,13,37], specific mechanisms about autophagosome formation and consequent mitophagy activation in response to inflammasome stimulators have not been studied. In my study, Sesn2 in conjunction with p62 plays a dual role to induce mitophagy activation to remove damaged mitochondria caused by stimulation with LPS and ATP. First, Sesn2 induces the perinuclear clustering of damaged mitochondria by mediating an aggregation of p62 and its recruitment to K63-linked ubiquitins on mitochondria surface. Second, Sestrin2 induces autophagosome formation, and consequent mitophagy through maintenance of ULK1 protein stability

The proper regulation of mitochondrial homeostasis at precise time points is critical because mitochondrial ROS generated by pathogen invasion at early times necessary to induce inflammasome activation to protect the host, but too much mitochondrial ROS caused by accumulation of damaged mitochondria could induce perpetual inflammasome activation, leading to chronic inflammation or apoptosis.

I presented a variety of evidence that Sesn2 induces mitophagy at a relatively late time (12 h) after stimulation with LPS and ATP, rather than at a relatively early time (6 h). First, the protein level of Sesn2, p62, and ULK1 were augmented at 12 h, rather than 6 h, after stimulation, and all of them were

fundamentally translocated into mitochondria at 12 h. Second, perinuclear clustering of damaged mitochondria was induced at 12 h after stimulation, and increased perinuclear clustering thereof had almost disappeared in both Sesn2$^{-/-}$ and p62$^{-/-}$ BMDMs. Third, the amounts of damaged mitochondria and consequent inflammasome activation were increased more highly in Sesn2$^{-/-}$ or p62$^{-/-}$ at 12 h after stimulation. Autophagy was induced at 6 h after treatment with LPS and ATP, as indicated by the observations that conversion of GFP-LC3-I to GFP-LC3-II were increased at 6 h after stimulation in my study (Figure 7A). However, autophagosome formation was not affected in Sesn2$^{-/-}$ at 6 h after stimulation, while activation of both autophagy and mitophagy were decreased in Sesn2$^{-/-}$ and p62$^{-/-}$ BMDMs at 12 h, indicating that Sesn2 in conjunction with p62 was required for autophagic activation and consequent mitophagy at 12 h after in response to LPS and ATP.

Several studies on the role of p62 in mitochondrial homeostasis have reported that p62 mediates the perinuclear aggregation of depolarized mitochondria generated by treatment with the mitochondria uncoupler, carbonyl cyanide m-chlorophenylhydrazone (CCCP) in neuronal cells, through interaction with polyubiquitinated proteins on damaged mitochondria [29-31]. In addition to a novel role of p62 for perinuclear clustering of damaged mitochondria by inflammasome stimulants via recruitment to K63-linked ubiquitines on mitochondria in my study, I also found that p62 induces autophagosome formation, as well as consequent mitophagy by use of p62$^{-/-}$ BMDMs. However, the mechanisms involved in mitophagic activation induced by p62 require further elucidation, although I have shown that they are not mediated by regulation of ULK1 stability nor ULK1 phosphorylation. Unlike the dual role of p62 in mitophagy, ULK1 was not involved in perinuclear clustering of damaged mitochondria upon stimulation, given that reduced perinuclear clustering of mitochondrdia in Sesn2$^{-/-}$ was not rescued by addition of human ULK1.

In spite of the inability of ULK1 to rescue perinuclear clustering of mitochondria in Sesn2$^{-/-}$, mitochondrial integrity was enhanced by rescue with ULK1 by increasing autophagic activity, suggesting that perinuclear clustering of damaged mitochondria might not always be required for mitophagic induction in BMDMs in response to LPS and ATP.

The translocation of Sesn2 and p62 into mitochondria might be induced by association of p62 with an unknown mitochondrial surface protein, rather than K63-linked ubiquitins on mitochondria, because Sesn2 is not required for translocation of p62 into mitochondria, but rather is responsible for the p62 recruitment to K63-linked ubiquitins on mitochondria surface. Sesn2 serves as an adapter protein that mediates p62's interaction with keap1 by interacting with p62 and keap1 simultaneously[18]. It was recently reported that Sesn2 also functions as a linker that promotes p62 phosphorylation by ULK1 via an interaction with ULK1 and p62, respectively[26]. These data support my results that Sesn2 induces perinuclear clustering of mitochondria via mediating p62's recruitment to K63-linked ubiquitins on damaged mitochondria. Although I did not identified K63-linked ubiquitinated proteins on mitochondria surface upon stimulation, Sesn2 might function as a scaffold protein that strengthens the otherwise weak association of p62 with them, leading to selective mitophagic processes.

Sesn2 has been reported to mediate autophagic activation under metabolic stress conditions through induction of AMPK activation[19], and ULK1 has been also reported to activate autophagy via its phosphorylation by AMPK[38]. However, AMPK activation was not affected, and ULK1 protein level was decreased in Sesn2$^{-/-}$ following stimulation. Rescue with ULK1 in Sesn2$^{-/-}$ BMDM recovered autophagy and mitopohagy activation, indicating that Sesn2 mediates autophagic activation independent of AMPK, and regulates autophagy through conservation of ULK1 protein stability, rather than ULK1 phosphorylation. In this context, I suggest that autophagic activation by Sesn2

in immune stimulation has distinct regulatory mechanisms, different from those in metabolic stress. Further research will be needed to identify the exact mechanisms whereby Sesn2 regulates the stability of ULK1 upon simulation.

Mitochondrial ROS generated from damaged mitochondria caused by inflammasome activators induce Sesn2 protein increase, and Sesn2 protein was augmented in monocytes having damaged mitochondria in septic shock patients. In this context, increased Sesn2 is essential for suppression of incessant inflammasome activation via removal of damaged mitochondria, because damaged mitochondria, IL-1β, and IL-18 were increased in $Sesn2^{-/-}$ BMDMs, and higher mortality, together with increased IL-1β, and IL-18, were observed in $Sesn2^{-/-}$ sepsis mouse models. Thus, Sesn2 might play a protective role for septic shock diseases via negative feedback regulation for mitochondria homeostasis.

V. CONCLUSION

Given these findings of the roles of Sesn2,p62 and ULK1 in mitophagic regulation in sepsis, I suggest that they may function in protective roles in other diseases caused by deregulation of mitophagy, including neurodegerative disorders, cardiovascular diseases, and cancer. Agents that increase protein level of Sesn2, p62 and ULK1 may provide beneficial effects through the improvement of mitochondrial quality.

REFERENCES

1. Franchi, L., Munoz-Planillo, R., Reimer, T., Eigenbrod, T., and Nunez, G. Inflammasomes as microbial sensors. Eur J Immunol 2010;40:611-5.
2. Schroder, K., and Tschopp, J. The inflammasomes. Cell 2010;140:821-32.
3. Gross, O., Thomas, C.J., Guarda, G., and Tschopp, J. The inflammasome: an integrated view. Immunol Rev 2011;243:136-51.
4. Latz, E., Xiao, T.S., and Stutz, A. Activation and regulation of the inflammasomes. Nat Rev Immunol 2013;13:397-411.
5. Rathinam, V.A., Vanaja, S.K., and Fitzgerald, K.A. Regulation of inflammasome signaling. Nat Immunol 2012;13:333-2.
6. Agostini, L., Martinon, F., Burns, K., McDermott, M.F., Hawkins, P.N., and Tschopp, J. NALP3 forms an IL-1beta-processing inflammasome with increased activity in Muckle-Wells autoinflammatory disorder. Immunity 2004;20:319-25.
7. Cerretti, D.P., Kozlosky, C.J., Mosley, B., Nelson, N., Van Ness, K., Greenstreet, T.A., March, C.J., Kronheim, S.R., Druck, T., Cannizzaro, L.A., et al. Molecular cloning of the interleukin-1 beta converting enzyme. Science 1992;256:97-100.
8. Cruz, C.M., Rinna, A., Forman, H.J., Ventura, A.L., Persechini, P.M., and Ojcius, D.M. ATP activates a reactive oxygen species-dependent oxidative stress response and secretion of proinflammatory cytokines in macrophages. J Biol Chem 2007;282:2871-9.
9. Zhou, R., Tardivel, A., Thorens, B., Choi, I., and Tschopp, J. Thioredoxin-interacting protein links oxidative stress to inflammasome activation. Nat Immunol 2010;11:136-40.

10. Misawa, T., Takahama, M., Kozaki, T., Lee, H., Zou, J., Saitoh, T., and Akira, S. Microtubule-driven spatial arrangement of mitochondria promotes activation of the NLRP3 inflammasome. Nat Immunol 2013;14:454-60.
11. Nakahira, K., Haspel, J.A., Rathinam, V.A., Lee, S.J., Dolinay, T., Lam, H.C., Englert, J.A., Rabinovitch, M., Cernadas, M., Kim, H.P., et al. Autophagy proteins regulate innate immune responses by inhibiting the release of mitochondrial DNA mediated by the NALP3 inflammasome. Nat Immunol 2011;12:222-30.
12. Shimada, K., Crother, T.R., Karlin, J., Dagvadorj, J., Chiba, N., Chen, S., Ramanujan, V.K., Wolf, A.J., Vergnes, L., Ojcius, D.M., et al. Oxidized mitochondrial DNA activates the NLRP3 inflammasome during apoptosis. Immunity 2012;36:401-14.
13. Zhou, R., Yazdi, A.S., Menu, P., and Tschopp, J. A role for mitochondria in NLRP3 i nflammasome activation. Nature 2011;469:221-5.
14. Saitoh, T., Fujita, N., Jang, M.H., Uematsu, S., Yang, B.G., Satoh, T., Omori, H., Noda, T., Yamamoto, N., Komatsu, M., et al. Loss of the autophagy protein Atg16L1 enhances endotoxin-induced IL-1beta production. Nature 2008;456:264-8.
15. Zhang, Z., Xu, X., Ma, J., Wu, J., Wang, Y., Zhou, R., and Han, J. Gene deletion of Gabarap enhances Nlrp3 inflammasome-dependent inflammatory responses. J Immunol 2013;190:3517-24.
16. Budanov, A.V., Sablina, A.A., Feinstein, E., Koonin, E.V., and Chumakov, P.M. Regeneration of peroxiredoxins by p53-regulated sestrins, homologs of bacterial AhpD. Science 2004;304:596-600.
17. Lee, J.H., Budanov, A.V., Park, E.J., Birse, R., Kim, T.E., Perkins,

G.A., Ocorr, K., Ellisman, M.H., Bodmer, R., Bier, E., et al. Sestrin as a feedback inhibitor of TOR that prevents age-related pathologies. Science 2010;327:1223-8

18. Bae, S.H., Sung, S.H., Oh, S.Y., Lim, J.M., Lee, S.K., Park, Y.N., Lee, H.E., Kang, D., and Rhee, S.G. Sestrins activate Nrf2 by promoting p62-dependent autophagic degradation of Keap1 and prevent oxidative liver damage. Cell Metab 2013;17:73-84.
19. Budanov, A.V., and Karin, M. p53 target genes sestrin1 and sestrin2 connect genotoxic stress and mTOR signaling. Cell 2008;134:451-60.
20. Chen, C.C., Jeon, S.M., Bhaskar, P.T., Nogueira, V., Sundararajan, D., Tonic, I., Park, Y., and Hay, N. FoxOs inhibit mTORC1 and activate Akt by inducing the expression of Sestrin3 and Rictor. Dev Cell 2010;18:592-604.
21. Lee, J.H., Budanov, A.V., Talukdar, S., Park, E.J., Park, H.L., Park, H.W., Bandyopadhyay, G., Li, N., Aghajan, M., Jang, I., et al. Maintenance of metabolic homeostasis by Sestrin2 and Sestrin3. Cell Metab 2012;16:311-21.
22. Park, H.W., Park, H., Ro, S.H., Jang, I., Semple, I.A., Kim, D.N., Kim, M., Nam, M., Zhang, D., Yin, L., et al. Hepatoprotective role of Sestrin2 against chronic ER stress. Nat Commun 2014;5:4233.
23. Mizushima, N., Yoshimori, T., and Levine, B. Methods in mammalian autophagy research. Cell 2010;140:313-26.
24. Li, P., Allen, H., Banerjee, S., Franklin, S., Herzog, L., Johnston, C., McDowell, J., Paskind, M., Rodman, L., Salfeld, J., et al. Mice deficient in IL-1 beta-converting enzyme are defective in production of mature IL-1 beta and resistant to endotoxic shock. Cell 1995;80:401-11.

25. Sutterwala, F.S., Ogura, Y., Szczepanik, M., Lara-Tejero, M., Lichtenberger, G.S., Grant, E.P., Bertin, J., Coyle, A.J., Galan, J.E., Askenase, P.W., et al. Critical role for NALP3/CIAS1/Cryopyrin in innate and adaptive immunity through its regulation of caspase-1. Immunity 2006;24:317-27.
26. Ro, S.H., Semple, I.A., Park, H., Park, H., Park, H.W., Kim, M., Kim, J.S., and Lee, J.H. Sestrin2 Promotes Unc-51-like Kinase 1 (ULK1)-Mediated Phosphorylation of p62/sequestosome-1. The FEBS journal 2014b.
27. Springer, W., and Kahle, P.J. Regulation of PINK1-Parkin-mediated mitophagy. Autophagy 2011;7:266-78.
28. Youle, R.J., and Narendra, D.P. Mechanisms of mitophagy. Nat Rev Mol Cell Biol 2011;12:9-14.
29. Geisler, S., Holmstrom, K.M., Skujat, D., Fiesel, F.C., Rothfuss, O.C., Kahle, P.J., and Springer, W. PINK1/Parkin-mediated mitophagy is dependent on VDAC1 and p62/SQSTM1. Nat Cell Biol 2010;12:119-31.
30. Narendra, D., Kane, L.A., Hauser, D.N., Fearnley, I.M., and Youle, R.J. p62/SQSTM1 is required for Parkin-induced mitochondrial clustering but not mitophagy; VDAC1 is dispensable for both. Autophagy 2010;6:1090-106.
31. Okatsu, K., Saisho, K., Shimanuki, M., Nakada, K., Shitara, H., Sou, Y.S., Kimura, M., Sato, S., Hattori, N., Komatsu, M., et al. p62/SQSTM1 cooperates with Parkin for perinuclear clustering of depolarized mitochondria. Genes Cells 2010;15:887-900.
32. Alers, S., Loffler, A.S., Wesselborg, S., and Stork, B. Role of AMPK-mTOR-Ulk1/2 in the regulation of autophagy: cross talk, shortcuts, and feedbacks. Mol Cell Biol 2012;32:2-11.
33. Kim, J., Kundu, M., Viollet, B., and Guan, K.L. AMPK and

mTOR regulate autophagy through direct phosphorylation of Ulk1. Nat Cell Biol 2011;13:132-41.

34. Shang, L., and Wang, X. AMPK and mTOR coordinate the regulation of Ulk1 and mammalian autophagy initiation. Autophagy 2011;7:924-6.
35. Budanov, A.V., and Karin, M. p53 target genes sestrin1 and sestrin2 connect genotoxic stress and mTOR signaling. Cell 2008;134:451-60.
36. Ro, S.H., Nam, M., Jang, I., Park, H.W., Park, H., Semple, I.A., Kim, M., Kim, J.S., Park, H., Einat, P., et al. Sestrin2 inhibits uncoupling protein 1 expression through suppressing reactive oxygen species. Proceedings of the National Academy of Sciences of the United States of America 2014a;111:7849-54.
37. Lupfer, C., Thomas, P.G., Anand, P.K., Vogel, P., Milasta, S., Martinez, J., Huang, G., Green, M., Kundu, M., Chi, H., et al. Receptor interacting protein kinase 2-mediated mitophagy regulates inflammasome activation during virus infection. Nat Immunol 2013;14:480-8.
38. Egan, D.F., Shackelford, D.B., Mihaylova, M.M., Gelino, S., Kohnz, R.A., Mair, W., Vasquez, D.S., Joshi, A., Gwinn, D.M., Taylor, R., et al. Phosphorylation of ULK1 (hATG1) by AMP-activated protein kinase connects energy sensing to mitophagy. Science 2011;331:456-61.

ABSTRACT(IN KOREAN)

미토파지를 유도함으로써 인플라마좀의 활성을 억제하는 세스트린2의 역할 규명

< 지도교수 유 지 환 >

연세대학교 대학원 의과학과

김 민 지

세포가 감염되었을 때 NLRP3 인플라마좀 복합체의 활성은 미토콘드리아가 생성하는 활성산소에 의해 유도되고, 오토파지에 의해 억제된다. 따라서 미토콘드리아의 온전성과 오토파지가 정교히 조절되어야만 적절한 인플라마좀 활성이 일어날 수 있다. 우리는 세포가 감염되었을 때 손상된 미토콘드리아의 축적에 의해 일어나는 NLRP3 인플라마좀의 활성을 억제하여 세포를 보호하는 세스트린2의 역할을 확인하였다. 세스트린2는 NLRP3 활성인자에 의해 손상되는 미토콘드리아를 제거하는 데 2가지 역할을 하였다. 첫번째로, 세스트린2는 미토콘드리아의 K63에 연결된 유비퀴틴과 p62와 상호작용하여 손상된 미토콘드리아가 핵 주변으로 모여들게 하였다. 두번째로, 세스트린2는 ULK1 단백질 레벨을 유지함으로써 오토파지와 미토파지를 유도하였다. 세스트린2가 결손된 쥐와 p62가 결손된

쥐는 패혈증 모델을 만들었을 때 IL-1β와 IL-18과 같은 Caspase-1과 관련된 사이토카인을 더 많이 분비하였고 사망률이 높았다. 이 연구를 통해 세스트린2가 미토콘드리아의 항상성을 유지하여 과도한 NLRP3 인플라마좀의 활성을 억제하는 역할을 한다는 것을 밝혀냈다.

핵심되는 말 : 세스트린2, p62, 미토파지, 오토파지